2021-07-29

Host tropism determination by convergent evolution of immunological evasion in the Lyme disease system

Thomas M. Hart
State University of New York at Albany

Et al.

PLOS PATHOGENS

RESEARCH ARTICLE

Host tropism determination by convergent evolution of immunological evasion in the Lyme disease system

Thomas M. Hart[1,2], Alan P. Dupuis, II[1], Danielle M. Tufts[3], Anna M. Blom[4], Simon R. Starkey[1], Ryan O. M. Rego[5,6], Sanjay Ram[7], Peter Kraiczy[8], Laura D. Kramer[1,9], Maria A. Diuk-Wasser[3], Sergios-Orestis Kolokotronis[10,11,12]*, Yi-Pin Lin[1,9]*

1 Division of Infectious Diseases, Wadsworth Center, New York State Department of Health, Albany, New York, United States of America, **2** Department of Biological Sciences, State University of New York at Albany, Albany, New York, United States of America, **3** Department of Ecology, Evolution, and Environmental Biology, Columbia University, New York, New York, United States of America, **4** Division of Medical Protein Chemistry, Department of Translational Medicine, Lund University, Malmo, Sweden, **5** Institute of Parasitology, Czech Academy of Sciences, České Budějovice, Czech Republic, **6** Faculty of Science, University of South Bohemia, České Budějovice, Czech Republic, **7** Division of Infectious Diseases and Immunology, University of Massachusetts Medical School, Worcester, Massachusetts, United States of America, **8** Institute of Medical Microbiology and Infection Control, University Hospital of Frankfurt, Goethe University Frankfurt, Frankfurt, Germany, **9** Department of Biomedical Sciences, State University of New York at Albany, Albany, New York, United States of America, **10** Department of Epidemiology and Biostatistics, School of Public Health, SUNY Downstate Health Sciences University, Brooklyn, New York, United States of America, **11** Institute for Genomic Health, SUNY Downstate Health Sciences University, Brooklyn, New York, United States of America, **12** Division of Infectious Diseases, Department of Medicine, College of Medicine, SUNY Downstate Health Sciences University, Brooklyn, New York, United States of America

* SOK@downstate.edu (S-OK); Yi-Pin.Lin@health.ny.gov (Y-PL)

Abstract

Pathogens possess the ability to adapt and survive in some host species but not in others–an ecological trait known as host tropism. Transmitted through ticks and carried mainly by mammals and birds, the Lyme disease (LD) bacterium is a well-suited model to study such tropism. Three main causative agents of LD, *Borrelia burgdorferi*, *B. afzelii*, and *B. garinii*, vary in host ranges through mechanisms eluding characterization. By feeding ticks infected with different *Borrelia* species, utilizing feeding chambers and live mice and quail, we found species-level differences in bacterial transmission. These differences localize on the tick blood meal, and specifically complement, a defense in vertebrate blood, and a polymorphic bacterial protein, CspA, which inactivates complement by binding to a host complement inhibitor, Factor H (FH). CspA selectively confers bacterial transmission to vertebrates that produce FH capable of allele-specific recognition. CspA is the only member of the Pfam54 gene family to exhibit host-specific FH-binding. Phylogenetic analyses revealed convergent evolution as the driver of such uniqueness, and that FH-binding likely emerged during the last glacial maximum. Our results identify a determinant of host tropism in Lyme disease infection, thus defining an evolutionary mechanism that shapes host-pathogen associations.

OPEN ACCESS

Citation: Hart TM, Dupuis AP, II, Tufts DM, Blom AM, Starkey SR, Rego ROM, et al. (2021) Host tropism determination by convergent evolution of immunological evasion in the Lyme disease system. PLoS Pathog 17(7): e1009801. https://doi.org/10.1371/journal.ppat.1009801

Editor: Jon T. Skare, Texas A&M University College Station: Texas A&M University, UNITED STATES

Received: April 30, 2021

Accepted: July 14, 2021

Published: July 29, 2021

Data Availability Statement: All relevant data are within the manuscript and its Supporting Information files.

Funding: This work was supported by NIH U01CK000509, NSF IOS1755370 (DMT and MDW), NSF IOS1754995 (SOK), NSF IOS1755286 (YPL, ADII, LDK, and TMH), DoD TB170111, NIH R21AI144891, NIH R21AI146381, New York State Department of Health Wadsworth Center Start-Up Grant (TMH and YPL), the Czech Science Foundation grant No. 17-21244S (ROMR), and the

LOEWE Center DRUID Novel Drug Targets against Poverty-Related and Neglected Tropical Infectious Diseases, project C3 (PK). The funders had no role in study design, data collection and analysis, decision to publish, or preparation of the manuscript.

Competing interests: The authors have declared that no competing interests exist.

Author summary

The evolution of pathogens in response to a host environment often leads to a specificity of these pathogens to survive in particular hosts, known as host tropism. However, the mechanisms of host tropism remain unclear. The Lyme disease (LD) bacterium is an ideal model to study such mechanisms because the causative agent of this disease (bacteria species) are transmitted by ticks and carried by multiple vertebrates, including mammals and birds. We found that different LD bacteria species vary in their ability to survive in mice and quail, and in ticks fed on human or quail blood after transmission. We also showed that such a variation is dependent on whether tick blood meals have functional complement, an innate defense in vertebrate blood. We attributed such species-to-species differences of transmission to the polymorphisms of a bacterial complement inactivating protein, CspA: CspA, by inactivating vertebrate complement in tick blood meals in a species-specific manner, allows bacterial transmission to selective vertebrates. We further demonstrated that this CspA-mediated bacterium species-specific complement evasion arose through convergent evolution, as an evolutionary mechanism to permit such vertebrate-bacteria interaction. The mechanisms defined in this multi-disciplinary work provide new insights into the host-pathogen interactions.

Introduction

The interactions between hosts and pathogens (e.g. bacteria, viruses, and protozoa) have arisen through numerous evolutionary events [1,2], often resulting in generalist pathogens, which adapt to most host environments, or specialists, which selectively survive in particular host species. The association between pathogens and their respective hosts is defined as "host tropism (or host specialization)" [3]. For vector-borne pathogens, such a host tropism can be dictated by not only host factors but also host constituents in the vectors (e.g. blood meals) [4]. Because many bacteria varying in host specificity are involved in the infection cycle, the Lyme disease bacterium is one of the models regularly applied to investigate the host-pathogen interactions [4]. Carried by *Ixodes* ticks, this disease is the most common vector-borne disease in the northern hemisphere [5]. The causative agent of Lyme disease is a genospecies complex of the spirochete *Borrelia burgdorferi* sensu lato (also known as *Borreliella burgdorferi* sensu lato (NCBI taxid: 139), Lyme borreliae) [6]. Among these genospecies, the most frequently isolated spirochetes from both ticks and vertebrate hosts are *B*. *afzelii*, *B*. *garinii*, and *B*. *burgdorferi* sensu stricto (hereafter referred to as *B*. *burgdorferi*) [7]. Following the tick bite, spirochetes need to survive in tick blood meals, which permit transmission to the bite site of the host skin. Survival in the host bloodstream then is a prerequisite for hematogenous dissemination and colonization of distant tissues, resulting in varied disease manifestations involving different organs in incidental hosts such as humans [8]. In nature, Lyme borreliae can invade vertebrate reservoirs (mainly birds and rodents) but varying in their ability to infect these animals in a host-specific manner [9,10]. For example, some Lyme borreliae species, such as *B*. *burgdorferi*, can invade a wide range of hosts whereas others are selectively infectious in few host taxa (e.g. *B*. *afzelii* for rodents and *B*. *garinii* for birds). However, the molecular basis for such host tropism is largely unclear [9,10].

The elimination of pathogens by host immune responses is a major bottleneck of infectivity, limiting the breadth of host competence [9,11,12]. Complement is one of the first lines of host defenses in vertebrate animals and can be activated through three canonical routes: the classical, lectin, and alternative pathways [13]. The activation of complement on the pathogen

surface results in the formation of a protein complex called C3 convertase. C3 convertase is essential for complement function because it serves as a protease to cleave C3 protein to its active fragments. Further complement activation leads to the lysis of pathogens due to the formation of membrane attack complex pores (C5b-9) on pathogen surfaces. C3 convertase formed by alternative pathway activation, called C3bBb (composed of C3b and Bb proteins), activates more C3 molecules and results in a positive feedback of the C3 amplification loop for the complement activation. To avoid tissue damage from unwanted complement activation in the absence of pathogens, hosts possess complement inhibitors [13,14]. One of these inhibitors is factor H (FH), which binds to C3b and blocks further activation of complement [13,15]. Like other pathogens, Lyme borreliae exploit such host self-regulatory mechanisms by recruiting complement inhibitors on their surface [10,16–18], which allows spirochetes to evade complement-mediated killing in the host bloodstream or tick blood meals [10,16–18]. In fact, spirochetes bind to FH through the production of several bacterial FH-binding proteins, called Complement Regulators Acquiring Surface Proteins (CRASPs): CspA, CspZ, and OspE-related proteins [19,20]. Among these CRASPs, CspA is uniquely required for bacterial transmission from nymphal ticks to vertebrate animals by binding to FH, resulting in complement evasion in those feeding ticks [21–23].

Interestingly, the ability of CspA to bind to FH from different vertebrate hosts varies by alleles and dictates the specificity of a Lyme borreliae species to survive in the sera of various animals [21,24,25]. Specifically, the ability of CspA variants to bind to mammalian FH and survive in homologous sera correlates with the ability of these variants to promote tick-to-mouse transmission [21]. These findings raise a possibility that CspA-mediated, FH binding-dependent complement evasion drives Lyme borreliae host tropism [9,10]. However, that possibility could not be fully demonstrated until we could elucidate the roles of CspA variants that do not promote tick-to-mouse transmission to confer tickborne transmission to other hosts. Additionally, if CspA is one of the spirochete determinants of host tropism, what evolutionary mechanisms give rise to the host-spirochete associations mediated by this protein?

In this study, we used Lyme disease spirochetes, avian and mammalian hosts, and the blood of mammals and birds as models to examine the role of complement in driving host tropism of pathogens. We further identified CspA as a molecular determinant for such tropism and elucidated the evolutionary mechanisms resulting in the allelically specific roles of this protein in conferring maintenance of pathogens in diverse hosts during the infection cycle.

Results

Lyme borreliae genospecies differ in their levels of transmission to wild-type but not complement-deficient mice and quail

To examine tick-to-host transmission among Lyme borreliae species, we intradermally injected wild-type BALB/c (wild-type; WT) mice with *B. burgdorferi* B31-5A4, *B. garinii* ZQ1, or *B. afzelii* CB43. The tissues from B31-5A4- or CB43-infected mice had significantly greater spirochete burdens than those from uninfected mice (S1A–S1D Fig). In contrast, except for the bladders from two mice, bacterial burdens in the tissues of ZQ1-infected mice were below detection limits (10 bacteria per 100ng total DNA) (S1A–S1D Fig). To generate ticks harboring equal loads of spirochetes, we intradermally injected each of these strains into C3-deficient BALB/c mice ($C3^{-/-}$) mice, which do not have functional complement. After allowing *I. scapularis* larvae to feed on these mice, we found similar burdens of these strains in all tested tissues, fed larvae, and post molting flat nymphs (S1E–S1J Fig).

We then permitted the nymphs carrying each of these strains to feed on WT mice and determined the spirochete burdens in the replete nymphs, the skin at the tick bite site, and

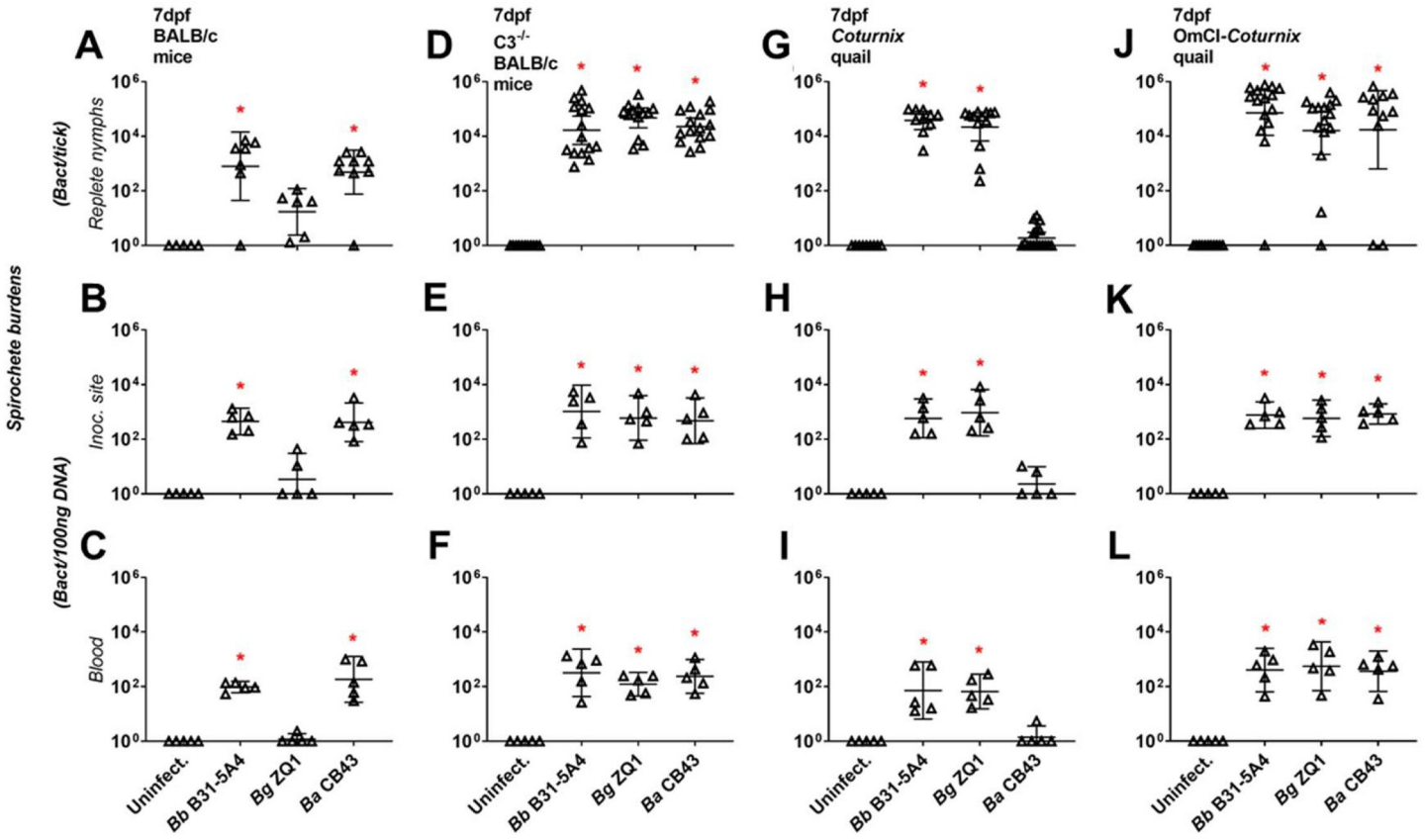

Fig 1. Lyme borreliae display species-level variation of tickborne transmission to wild-type but not complement-deficient mice and quail. *Ixodes scapularis* nymphs infected with *B. burgdorferi* B31-5A4 ("*Bb* B31-5A4"), *B. garinii* ZQ1 ("*Bg* ZQ1"), or *B. afzelii* CB43 ("*Ba* CB43") fed on **(A-C)** BALB/c mice, **(D-F)** $C3^{-/-}$ BALB/c mice, **(G-I)** *Coturnix* quail, or **(J-L)** OmCI-treated *Coturnix* quail. Uninfected nymphs and mouse and quail tissues were included as control ("Uninfect."). Fed nymphs were collected upon repletion, and blood and the tick bite sites of skin were collected at 7 days post nymph feeding ("dpf"). Spirochete burdens in **(A, D, G, and J)** replete nymphs, **(B, E, H, and K)** tick bite site of skin ("Inoc. site"), and **(C, F, I, and L)** blood were determined by qPCR. For the burdens in tissue and blood samples, the resulting values were normalized to 100 ng total DNA. Shown are the geometric means of bacterial loads ± 95% confidence interval of bacterial burdens in tissues and blood from 5 mice or quail per group or nymphs feeding on mice (7 nymphs carrying *Bb* B31-5A4, 6 nymphs carrying *Bg* ZQ1, or 9 nymphs carrying *Ba* CB43), $C3^{-/-}$ mice (15 nymphs carrying *Bb* B31-5A4 or *Bg* ZQ1, or 13 nymphs carrying *Ba* CB43), quail (10 nymphs carrying *Bb* B31-5A4, 13 nymphs carrying *Bg* ZQ1, or 17 nymphs carrying *Ba* CB43), or OmCI-treated quail (15 nymphs carrying *Bb* B31-5A4, 11 nymphs carrying *Bg* ZQ1, or 15 nymphs carrying *Ba* CB43). Significant differences ($p < 0.05$, Kruskal-Wallis test with the two-stage step-up method of Benjamini, Krieger, and Yekutieli) in the spirochete burdens relative to uninfected ticks or tissues are indicated with an asterisk.

https://doi.org/10.1371/journal.ppat.1009801.g001

blood from these animals at 7 days post feeding (dpf), and uninfected nymphs were included as control. Strains B31-5A4 and CB43 survived at these sites (~10^3 spirochetes per tick or 10^2 to 10^3 spirochetes per 100ng DNA of tissues, Fig 1A–1C). Two out of six fed nymphs had undetectable loads of ZQ1 whereas the other four ticks have bacterial loads ranging from 39 to 111 spirochetes per tick (Fig 1A). These low, variable values were not significantly different compared to uninfected nymphs (Fig 1A, $p = 0.52$). Strain ZQ1 was also largely undetectable in tick bite sites and blood (three and five out of five bite sites and blood samples, respectively; Fig 1B and 1C). Additionally, we fed nymphs carrying B31-5A4, CB43, or ZQ1 on $C3^{-/-}$ mice and found that these strains were detected in fed nymphs, bite sites, and blood at similar levels (Fig 1D–1F). These results indicate that ZQ1 is less capable of surviving in fed nymphs and establishing infection than B31-5A4 and CB43 after ticks fed only on WT mice, but not on the mice lacking C3, suggesting that mouse complement dictates spirochete transmission. We further studied the tickborne transmission of these strains in a similar fashion using *Coturnix*

quail, the avian model of Lyme disease [26,27]. We detected B31-5A4 and ZQ1 in fed nymphs, tick bite sites, and bloodstream (~10^4 spirochetes per tick or 10^2 to 10^3 Lyme borreliae per 100ng DNA of tissues, Fig 1G–1I). Conversely, strain CB43 was not detected above the detection limit in these ticks and tissue samples (Fig 1G–1I). The nymphs carrying each of these strains were then allowed to feed on quail treated with *O. moubata* complement inhibitor (OmCI), which is the only tick salivary protein reported to block quail and other avian complement at the level of C5 activation (S2 Fig)[28]. We found similar levels of spirochetes in fed nymphs, tick bite sites and blood (Fig 1J–1L). These data showed less efficient tick-to-quail transmission of CB43 than that of B31-5A4 and ZQ1, and as was the case in mice, quail complement dictates transmission efficiency among those spirochete strains.

The different abilities of Lyme borreliae genospecies to evade complement in tick blood meals determine mammalian- or avian-specific spirochete transmission

To examine the role that the source of the blood meals plays in determining spirochete transmission, nymphs infected with B31-5A4, ZQ1, or CB43 were allowed to feed on artificial feeding chambers with human blood, the mammalian blood representative [29](Fig 2A). Uninfected nymphs were included as controls. We did not detect statistical difference of the number of attached ticks feeding on quail blood, compared to those on human blood, consistent with our previous study [29]. We found that B31-5A4 and CB43 survive in fed nymphs and blood (~10^3 spirochetes per tick and 10^2 spirochetes per 100ng DNA of blood, Fig 2B and 2C). In contrast, ZQ1 was undetectable in the majority of human blood-fed nymphs (6 out of 10 ticks) (Fig 2B). Similarly, none of the blood samples fed on by ZQ1-infected nymphs had spirochete burdens significantly greater than uninfected blood (Fig 2C). We also allowed nymphs carrying B31-5A4, ZQ1, or CB43 to feed on human blood treated with Cobra Venom Factor (CVF), which depletes human complement cascade from the level of C3 [30]. We found similar burdens of these strains in the fed nymphs and the blood samples (~10^3 spirochetes per tick and ~10^2 spirochetes per 100ng DNA of blood, Fig 2D and 2E). These results indicate that ZQ1 is less competent than B31-5A4 or CB43 to survive in the tick blood meals from humans during transmission, and active human complement in the blood meals drives survival differences. We also performed similar work using quail blood and detected the strains B31-5A4 and ZQ1 in fed nymphs and blood (~10^3 spirochetes per tick and ~10^2 spirochetes per 100ng total DNA of blood, Fig 2F and 2G). However, the strain CB43 was not detected in the majority of fed nymphs (7 out of 13 nymphs, Fig 2F; $P > 0.05$ compared to uninfected nymphs). Further, spirochete burden values in blood samples fed on by nymphs carrying CB43 were indistinguishable from those of uninfected blood samples (Fig 2G). Similar levels of each strain were observed when nymphs carrying each of these strains were fed on OmCI-treated quail blood (~10^3 spirochetes per tick and 10^2 spirochetes per 100ng DNA of blood, Fig 2H and 2I). These findings indicate that quail complement limits CB43 survival when ticks feed on quail blood.

CspA-mediated quail FH-binding activity promotes tick-to-quail transmission of spirochetes by complement evasion

We previously showed that a *cspA*-deficient mutant *B. burgdorferi* producing a spirochete outer surface protein, CspA, from the *B. burgdorferi* B31 ($CspA_{B31}$) or *B. afzelii* PKo ($CspA_{PKo}$) but not from *B. garinii* ZQ1 ($CspA_{ZQ1}$), facilitates tick-to-mouse transmission by surviving in fed nymphs [21]. This isogenic strain-specific transmission is dependent on the mouse FH-binding activity of these CspA variants to evade complement [21] (S1 Table) and recapitulates

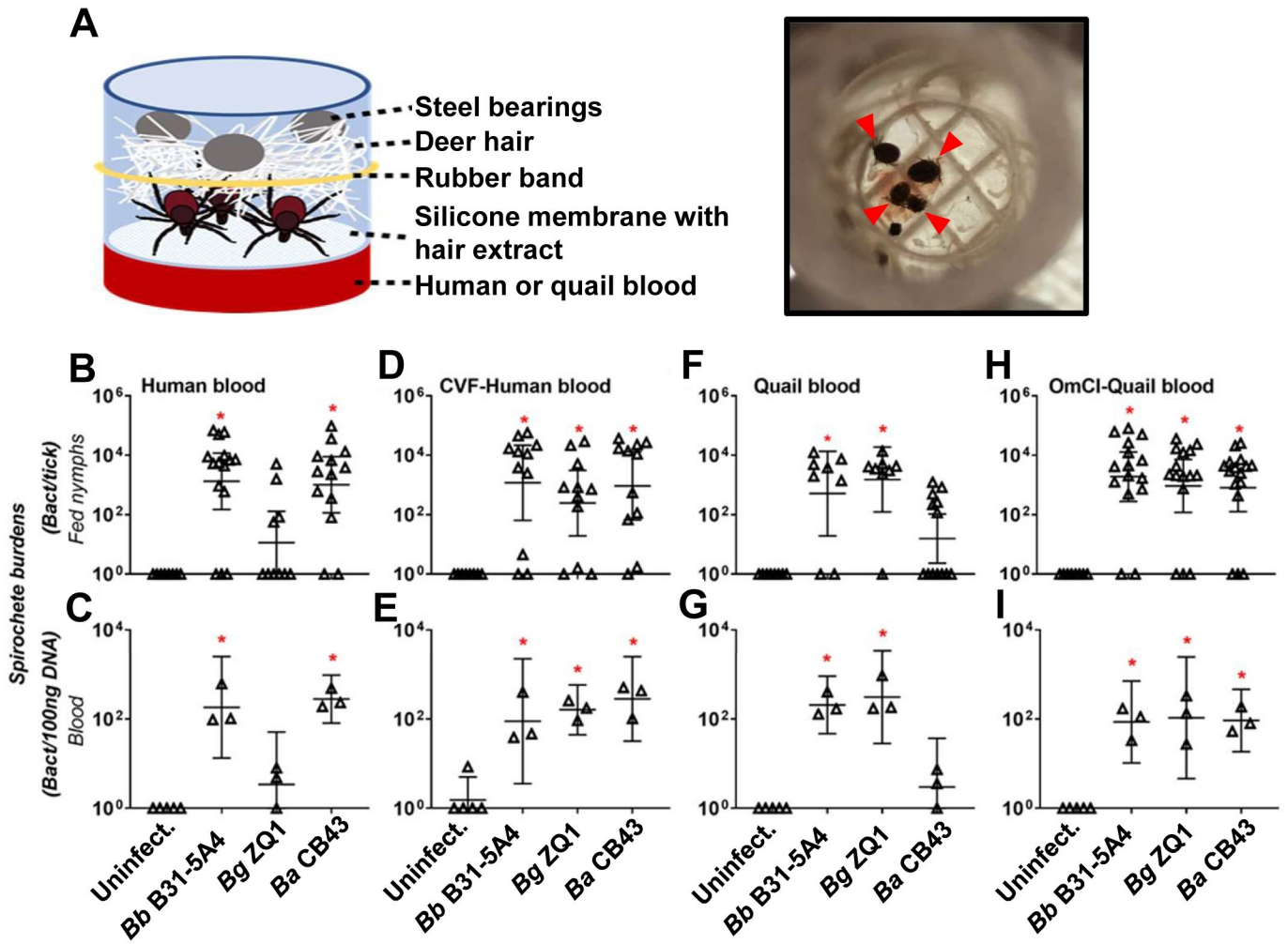

Fig 2. Complement in tick blood meals determines human or quail blood-specific spirochete transmission in feeding chambers. (A) (left panel) The schematic diagram showing the artificial feeding chamber that is used to examine the tickborne spirochete transmission in this study. **(Right panel)** The picture showing the engorged *I. scapularis* nymphs (indicated by arrows) in the chamber feeding on OmCI-treated quail blood. **(B-I)** *I. scapularis* nymphs infected with *B. burgdorferi* B31-5A4 ("*Bb* B31-5A4"), *B. garinii* ZQ1 ("*Bg* ZQ1"), or *B. afzelii* CB43 ("*Ba* CB43"), were allowed to feed in artificial feeding chambers submerging into six well plates containing **(B and C)** untreated or **(D and E)** CVF-treated human blood, or **(F and G)** untreated or **(H and I)** OmCI-treated quail blood. Blood was changed every 24-h and collected along with ticks on the fifth day of feeding. Uninfected nymphs and blood were included as control ("Uninfect."). Spirochete burdens in **(B, D, F, and H)** fed nymphs and **(C, E, G, and I)** blood were determined by qPCR. The spirochete burdens in the blood were obtained by normalizing the resulting values to 100 ng total DNA. Shown are the geometric means of bacterial loads ± 95% confidence interval of bacterial burdens from the 3 human or quail blood samples or nymphs feeding on untreated human blood (15 nymphs carrying *Bb* B31-5A4, 10 nymphs carrying *Bg* ZQ1, or 13 nymphs carrying *Ba* CB43), CVF-treated human blood (11 nymphs carrying *Bb* B31-5A4, *Bg* ZQ1, or *Ba* CB43), quail blood (8 nymphs carrying *Bb* B31-5A4 or *Bg* ZQ1 or 13 nymphs carrying *Ba* CB43), or OmCI-treated quail blood (15 nymphs carrying *Bb* B31-5A4 or *Bg* ZQ1 or 16 nymphs carrying *Ba* CB43). Significant differences ($p < 0.05$, Kruskal-Wallis test with the two-stage step-up method of Benjamini, Krieger, and Yekutieli) in the spirochete burdens relative to uninfected ticks or blood are indicated with an asterisk.

https://doi.org/10.1371/journal.ppat.1009801.g002

the mouse-specific tickborne transmissibility of *B. burgdorferi* B31, *B. afzelii* CB43, and *B. garinii* ZQ1 (Fig 1). Note that CspA from *B. afzelii* CB43 ($CspA_{CB43}$) shares 99% amino acid identity with $CspA_{PKo}$, making these CspA variants likely confer similar FH-binding and transmission phenotypes (S3A Fig). To extend that isogenic strain-specific phenotype to other small mammals, we allowed nymphs carrying the *cspA*-deficient *B. burgdorferi* producing $CspA_{B31}$, $CspA_{PKo}$, or $CspA_{ZQ1}$ to feed on a rodent reservoir of Lyme borreliae, *Peromyscus leucopus*. We found that expression of $CspA_{B31}$ and $CspA_{PKo}$, but not $CspA_{ZQ1}$, permitted spirochete transmission to that rodent species (S4 Fig). Further, our previous findings of $CspA_{ZQ1}$

(and $CspA_{B31}$) binding to quail FH and promoting survival in quail serum raised the hypothesis that CspA variants that bound FH drives tick-to-quail transmission [21] (S1 Table). To test this hypothesis, quail were fed on by the nymphs carrying WT *B. burgdorferi* B31-5A15 (5A15), *B. burgdorferi* B31-5A4NP1Δ*cspA* harboring an empty vector (Δ*cspA*/Vector), or the *cspA*-deficient strain carrying plasmids to express $CspA_{B31}$, $CspA_{ZQ1}$, or $CspA_{PKo}$ in the background of B31-5A4NP1Δ*cspA*. We also included an isogenic strain producing $CspA_{B31}$-L246D. This mutant protein is derived from $CspA_{B31}$ and selectively devoid of quail FH-binding activity but retaining other previously reported ligand-binding activities of CspA and thus can be used as negative control as a FH-binding deficient variant [21,31](S1 Table). Uninfected ticks were included as control. The strain 5A15 but not Δ*cspA*/Vector or $cspA_{B31}$-L246D-complemented strain, had burdens above detection limits in the fed nymphs, tick bite sites and blood (Fig 3A–3C). Strains producing $CspA_{B31}$ or $CspA_{ZQ1}$ but not $CspA_{PKo}$, had detectable burdens in the fed nymphs or tick bite sites and blood (~10^4 spirochetes per tick and ~10^2 spirochetes per 100ng DNA of tissues or blood, Fig 3A–3C). In contrast, when nymphs carrying each of these spirochete strains were permitted to feed on OmCI-treated quail, all strains showed comparable burdens in fed nymphs, tick bite sites, and blood (Fig 3D–3F). These findings suggest that the $CspA_{ZQ1}$ and $CspA_{B31}$ as quail FH binders promote tick-to-quail transmission by evading complement, and CspA-mediated quail FH-binding activity dictates such a transmission.

Allelically variable, CspA-mediated FH-binding activity confers spirochete complement evasion in tick blood meals and transmissibility in a mammalian and avian blood-specific manner

We sought to examine whether CspA-mediated FH-binding activity facilitates spirochete evasion of complement in tick blood meals, and if that ability determines tickborne transmission in a host-specific manner. Human blood was allowed to be ingested by the nymphs carrying 5A15, Δ*cspA*/Vector, or this strain producing $CspA_{B31}$, $CspA_{ZQ1}$, $CspA_{PKo}$, or $CspA_{B31}$-L246D using feeding chambers. We detected 5A15, but not Δ*cspA*/Vector or $CspA_{B31}$-L246D-producing strains, in fed nymphs and blood (Fig 4A and 4B). The $CspA_{B31}$- or $CspA_{PKo}$-producing strains were found in fed nymphs and in human blood (~10^4 spirochetes per tick (Fig 4A) and more than 10 spirochetes per 100ng total DNA of blood (Fig 4B)). Conversely, the $CspA_{ZQ1}$-producing strain was not detectable in these samples (Fig 4A and 4B). When we allowed nymphs carrying the same strains to feed on CVF-treated human blood, all strains were detected at similar burdens in fed nymphs and blood (Fig 4C and 4D). These results suggest that $CspA_{B31}$ and $CspA_{PKo}$, but not $CspA_{ZQ1}$, permitted transmission to human blood by facilitating human FH-binding mediated complement evasion in tick blood meals. We also permitted the nymphs carrying the above-mentioned strains to feed on quail blood in the same fashion and found B31-5A15, but not Δ*cspA*/Vector or $CspA_{B31}$-L246D, in the fed nymphs and blood had detectable burdens in both nymphs and blood (Fig 4E and 4F). The $CspA_{B31}$- or $CspA_{ZQ1}$-producing strain was readily detected in fed nymphs and blood (Fig 4E and 4F). Though three and two ticks carrying the $CspA_{PKo}$ and $CspA_{B31}$-L246D-producing strain, respectively, had burdens greater than detection limits, we did not detect any spirochetes in the remaining 10 nymphs (Fig 4E). Additionally, the burdens of these strains in the blood were statistically indistinguishable from uninfected blood samples (Fig 4F). When we performed similar experiments using OmCI-treated quail blood, all strains were found in nymphs and blood at comparable levels (Fig 4G and 4H). These results show the contribution of quail FH-binding dependent complement evasion in tick blood meals in promoting transmission to quail blood, and $CspA_{B31}$ and $CspA_{ZQ1}$, but not $CspA_{PKo}$, conferred these activities.

CspA homologs showed discontinuous sequence variation and genospecies-specific polymorphisms

Given the finding that homologous CspA proteins from single strains of *B. burgdorferi*, *B. afzelii*, or *B. garinii* confer distinct host tropism, we examined CspA variation in publicly available

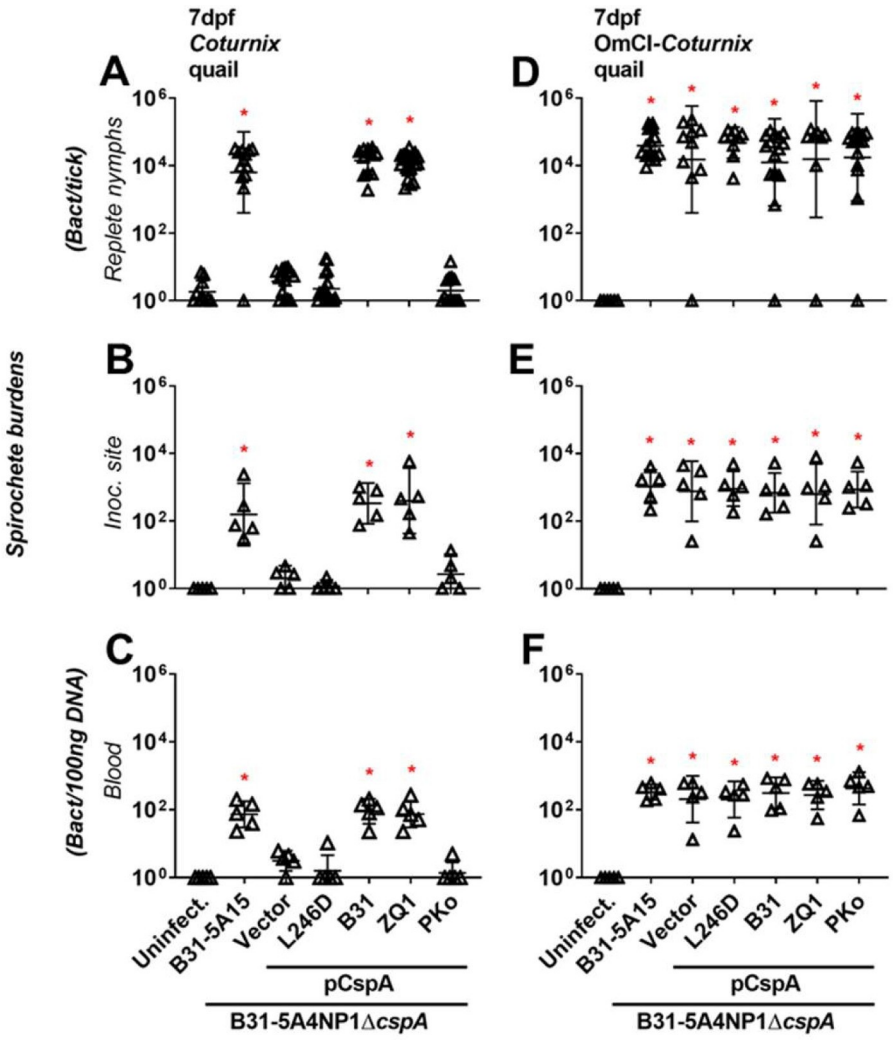

Fig 3. Polymorphic quail FH-binding activity of CspA confers the distinct transmissibility of Lyme borreliae to quail. *Ixodes scapularis* nymphs infected with WT *B. burgdorferi* B31-5A15 ("B31-5A15"), *B. burgdorferi* B31-5A4NP1Δ*cspA* transformed with an empty shuttle vector ("Vector"), or this deletion strain producing a mutated variant of CspA from *B. burgdorferi* B31 selectively devoid of quail FH binding activity ("L246D"), WT *B. burgdorferi* B31 ("B31"), *B. garinii* ZQ1 ("ZQ1"), or *B. afzelii* PKo ("PKo") were allowed to feed on **(A-C)** untreated or **(D-F)** OmCI-treated quail. Uninfected nymphs and quail tissues were included as control ("Uninfect."). Fed nymphs were collected upon repletion, and blood and tissues were collected at 7 days post nymph feeding ("dpf"). Spirochete burdens in **(A and D)** replete nymphs, **(B and E)** tick bite sites of skin ("Inoc. site"), and **(C and F)** blood were determined by qPCR. For the burdens in tissue samples, the resulting values were normalized to 100ng total DNA. Shown are the geometric means of bacterial loads ± 95% confidence interval of bacterial burdens from 5 quail tissues and blood or nymphs feeding on untreated quail (13 nymphs carrying the strains B31-5A15 or pCspA-PKo, 15 nymphs carrying the strains "Vector", 12 nymphs carrying the strain pCspA-B31, 21 nymphs carrying the strain pCspA-ZQ1, or 17 nymphs carrying the strain pCspA-L246D), or the nymphs from OmCI-treated quail (15 nymphs carrying the strains B31-5A15, pCspA-B31, or pCspA-PKo, 8 nymphs carrying the strains "Vector", 9 nymphs carrying the strain pCspA-L246D, 8 nymphs carrying the strain pCspA-ZQ1). Significant differences ($p < 0.05$, Kruskal-Wallis test with the two-stage step-up method of Benjamini, Krieger, and Yekutieli) in the spirochete burdens relative to uninfected ticks or quail tissues are indicated with an asterisk.

https://doi.org/10.1371/journal.ppat.1009801.g003

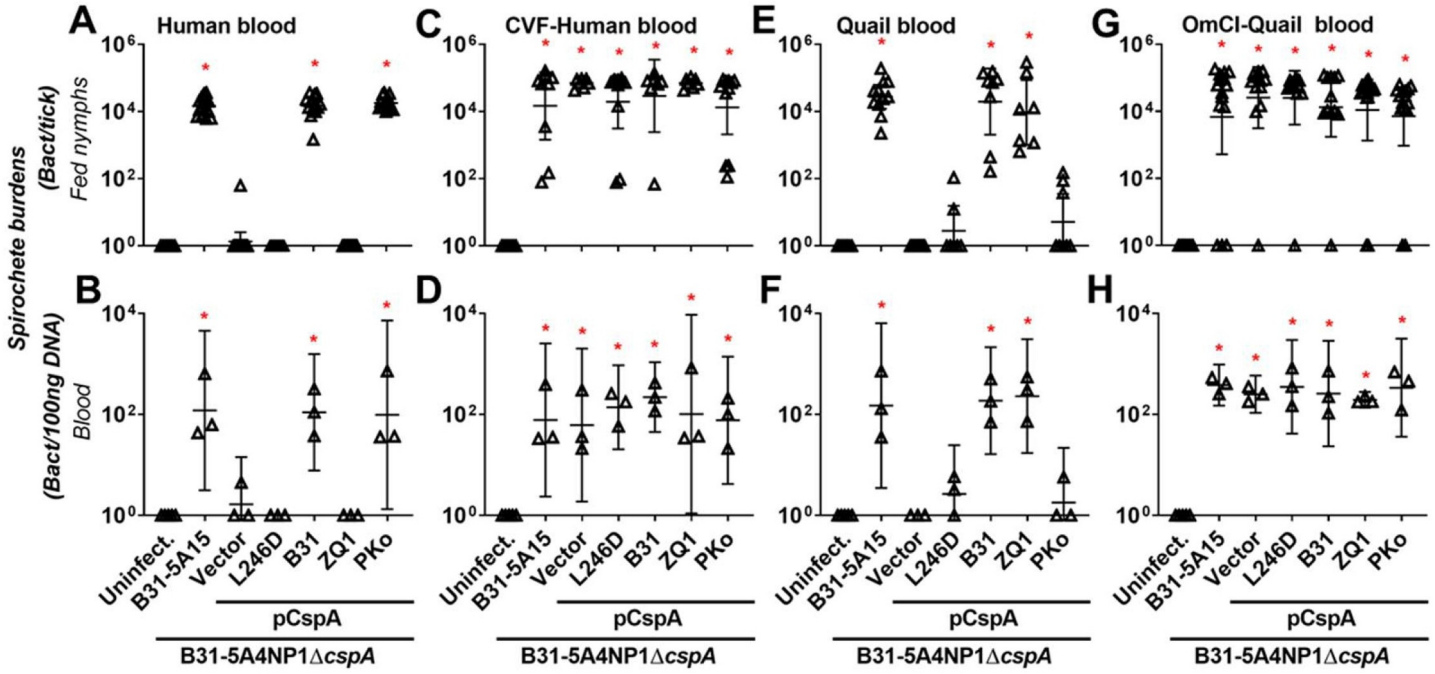

Fig 4. Allelically variable FH-binding activity of CspA dictates human- and quail blood-specific transmission in feeding chambers by evading complement in tick blood meals. *I. scapularis* nymphs infected with WT *B. burgdorferi* B31-5A15 ("B31-5A15"), *B. burgdorferi* B31-5A4NP1*ΔcspA* transformed with an empty shuttle vector ("Vector"), or this deletion strain transformed to produce a mutated variant of CspA from *B. burgdorferi* B31 selectively devoid of FH binding activity ("L246D"), WT *B. burgdorferi* B31 ("B31"), *B. garinii* ZQ1 ("ZQ1"), or *B. afzelii* PKo ("PKo") were allowed to feed in feeding chambers submerged into 6-well plates containing **(A and B)** untreated or **(C and D)** CVF-treated human blood, or **(E and F)** untreated or **(G and H)** OmCI-treated quail blood. Blood was changed every 24-h and was collected along with ticks on the fifth day of feeding. Uninfected nymphs and blood were included as control ("Uninfect."). Spirochete burdens from **(A, C, E and G)** fed nymphs and **(B, D, F, and H)** blood were determined by qPCR. For the burdens in tissue samples, the resulting values were normalized to 100ng total DNA. Shown are the geometric means of bacterial loads and 95% confidence interval of bacterial burdens from 3 human and quail blood samples, or nymphs feeding on untreated human blood (15 nymphs carrying the strains B31-5A15 or pCspA-B31, 14 nymphs carrying the strains "Vector" or pCspA-PKo, 17 nymphs carrying the strain pCspA-L246D, or 16 nymphs carrying the strain pCspA-ZQ1), or CVF-treated human blood (9 nymphs carrying the strain B31-5A15, 7 nymphs carrying the strains "Vector", pCspA-B31, or pCspA-ZQ1, or 11 nymphs carrying the strains pCspA-L246D or pCspA-PKo), untreated quail blood (11 nymphs carrying the strains B31-5A15 or "Vector", 8 nymphs carrying the strains pCspA-B31 or pCspA-PKo, or 7 nymphs carrying the strains pCspA-ZQ1 or pCspA-L246D) or OmCI-treated quail blood (15 nymphs carrying the strains B31-5A15, pCspA-PKo, or pCspA-ZQ1, 12 nymphs carrying the strains "Vector" or pCspA-B31, or 13 nymphs carrying the strain pCspA-L246D). Significant differences ($p < 0.05$, Kruskal-Wallis test with the two-stage step-up method of Benjamini, Krieger, and Yekutieli) in the spirochete burdens relative to uninfected ticks or quail tissues are indicated with an asterisk.

https://doi.org/10.1371/journal.ppat.1009801.g004

sequences. CspA is nested in the fourth clade of a protein family encoded on the linear plasmid 54, lp54 (PFam54-IV) (41–81% nucleotide identity; Fig 5A) [32,33]. However, the homology of all PFam54-IV proteins makes it difficult to identify CspA variants, leading to inaccurate annotations and misidentification [32]. We thus compiled publicly available gene sequences encoding PFam54-IV available in GenBank from *B. burgdorferi*, *B. afzelii*, and *B. garinii*, and compared the pairwise nucleotide identities of codon alignments for these genes from each species. Within PFam54-IV-encoding genes of any one particular *B. burgdorferi* strain, we identified one-to-one orthologous genes based on sequence conservation (>95% identity, green in S5 Fig). In contrast, we found moderate conservation among PFam54-IV homologs lacking such one-to-one orthology (<81% identity, red and yellow in S5 Fig). Sequence divergence patterns (inlets in S5–S7 Figs) allowed us to identify genes encoding $CspA_{B31}$, $CspA_{PKo}$, and $CspA_{ZQ1}$ as CspA orthologs in *B. burgdorferi*, *B. afzelii*, and *B. garinii*, respectively. Among these CspA orthologs, intraspecific diversity (i.e. within genospecies) exceeded 93% identity, while interspecific diversity (i.e. between genospecies) ranged from 67 to 72% (Fig 5B and 5C). These results suggest a genospecies-specific polymorphism among CspA variants,

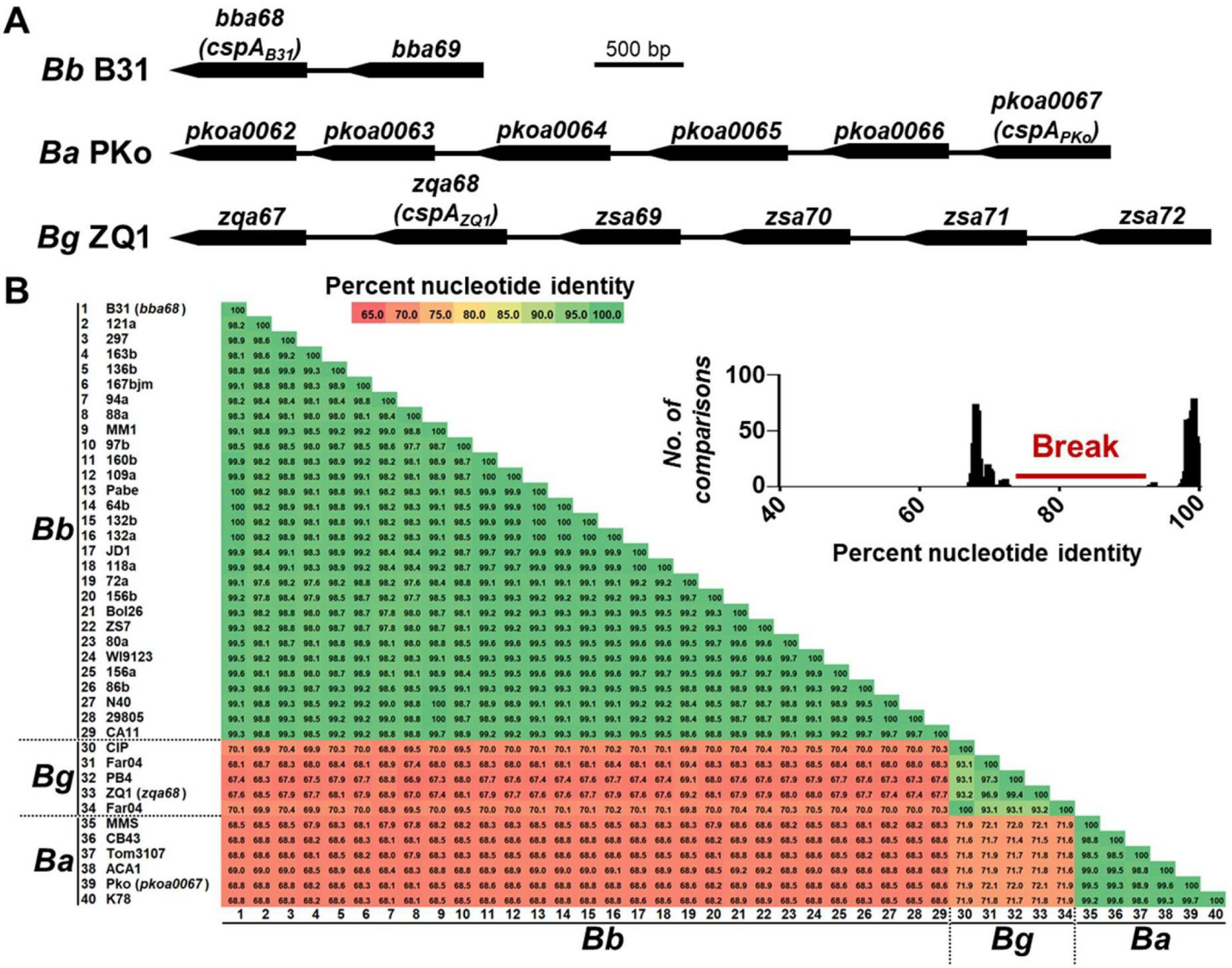

Fig 5. Genetic divergence in CspA variants across *B. burgdorferi* B31, *B. afzelii* PKo, and *B. garinii* ZQ1. (A) Synteny of Pfam54-IV loci in *B. burgdorferi* B31, *B. afzelii* PKo, and *B. garinii* ZQ1 **(B)** Pairwise nucleotide identity across the three spirochete species. **(inset)** Frequency distribution of pairwise genetic distances. The pairwise identity numbers are coded by color gradually from identical (100% pairwise identity; green) to divergent sequences (65% pairwise identity; red). The clear break in the frequency distribution separates the highly similar (> 95% pairwise identity) from moderately divergent comparisons (< 80%).

https://doi.org/10.1371/journal.ppat.1009801.g005

whereby variants of the same genospecies share notably high identity, and variants of different genospecies share relatively lower identities.

Host-specific FH-binding activity of CspA variants arose through convergent evolution

An average identity of 74% among the genes encoding CspA and other Pfam54-IV proteins raises the possibility that non-CspA members of Pfam54-IV share FH-binding functions. We thus examined the mouse (*Mus musculus*) and quail FH-binding ability of Pfam54-IV from *B. burgdorferi* B31-5A4, *B. afzelii* MMS, and *B. garinii* ZQ1 using ELISA. Note that PFam54-IV members from *B. afzelii* MMS, PKo, and CB43 are nearly identical (>99% identity) (S3A and

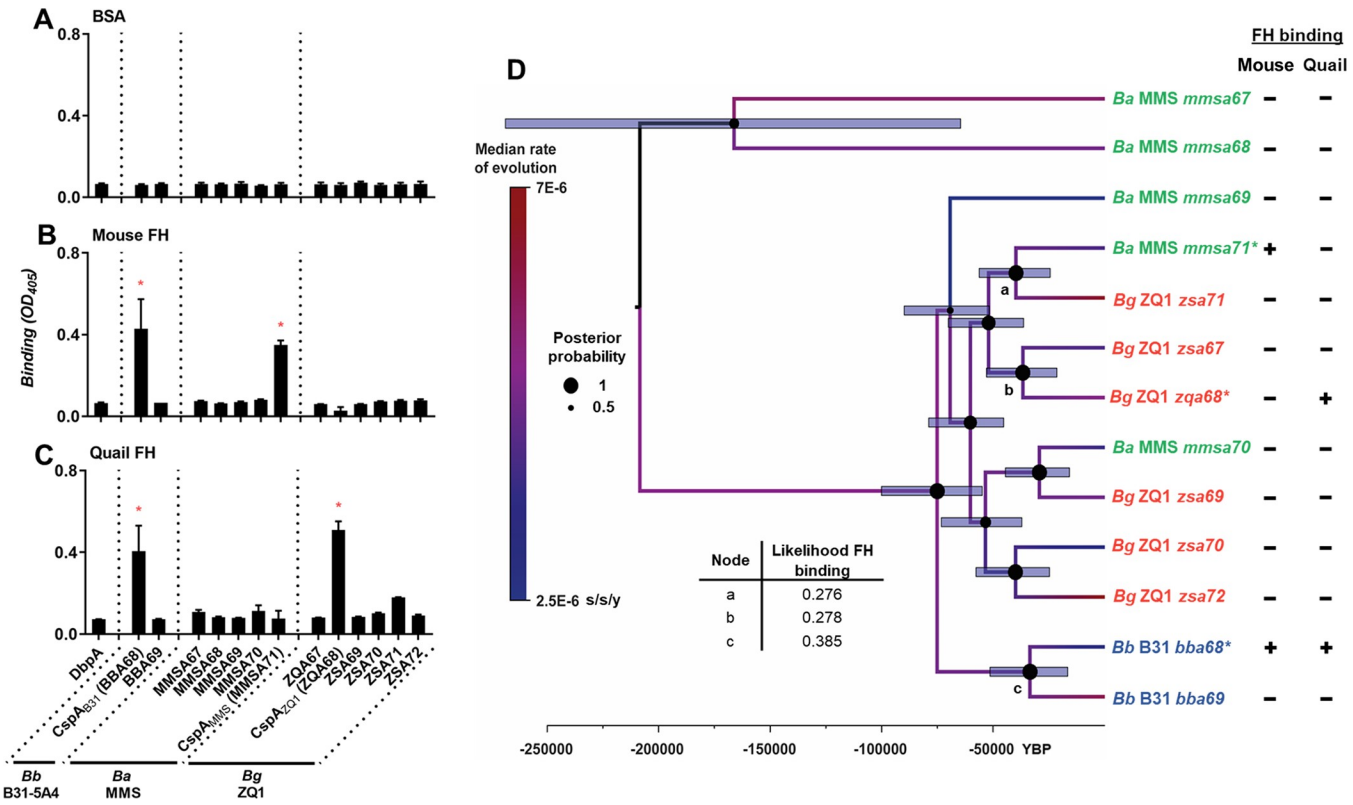

Fig 6. Allelically variable, host-specific FH-binding activity of CspA has emerged from convergent evolution. (A to C) Two μM of histidine-tagged Pfam54-IV proteins from *B. burgdorferi* B31-5A4, *B. afzelii* PKo, or *B. garinii* ZQ1 or recombinant histidine-tagged DbpA from *B. burgdorferi* B31-5A4 (negative control) were added in triplicate to wells coated with of purified **(A)** BSA (negative control) or **(B)** mouse or **(C)** quail FH. Protein binding was measured by ELISA in three independent experiments. Each bar represents the geometric mean ± 95% confidence interval of three replicates in one representative experiment. Significant differences ($p < 0.05$, Kruskal-Wallis test with the two-stage step-up method of Benjamini, Krieger, and Yekutieli) in the levels of FH binding of indicated proteins relative to DbpA are indicated (*). The ability of each protein in binding to factor H is summarized in S1 Table. **(D)** Maximum clade credibility tree is based on Pfam54-IV genes from *B. burgdorferi* B31 (blue), *B. afzelii* MMS (green), *B. garinii* ZQ1 (red). The scale bar represents an approximate timeline of evolution, in years before present ("YBP"), using the estimated substitution rate of 4.75×10^{-6} substitutions/site/year. Node bars represent the 95% highest posterior density of the node age. Node circles represent the posterior probability support. Branches are colored based on estimated the median substitution rate as per the legend to the left. Maximum likelihood- and parsimony-based ancestral state reconstructions were used to estimate FH-binding activities at ancestral nodes.

https://doi.org/10.1371/journal.ppat.1009801.g006

S6 Figs). We used Pfam54-IV of MMS to represent these proteins of *B. afzelii* given that the recombinant version of these proteins from MMS had been generated in our previous work [24]. As expected, PFam54-IV from *B. burgdorferi* B31-5A4, *B. afzelii* MMS, and *B. garinii* ZQ1 did not bind to BSA (Fig 6A). We found that CspA$_{B31}$ and CspA$_{MMS}$ bound to mouse FH at levels greater than a negative control spirochete protein, DbpA [21] (Fig 6B). Despite a high concentration (2μM) of other recombinant Pfam54-IV used, none bound to mouse FH over baseline levels seen with DbpA (Fig 6B). Furthermore, we observed that CspA$_{B31}$ and CspA$_{ZQ1}$, but none of other tested Pfam54-IV, bound to quail FH (Fig 6C). These results indicate that the host-specific and allelically variable FH-binding activity of Pfam54-IV is CspA-dependent.

To further study the evolutionary mechanisms leading to host-specific and allelically variable FH-binding activity of CspA, we estimated the phylogenetic relationships among gene sequences encoding PFam54-IV from *B. burgdorferi* B31, *B. afzelii* MMS, and *B. garinii* ZQ1. We found that those sequences of the same genospecies do not form monophyletic assemblages, but CspA variants grouped in separate clades with moderate to high internode branch

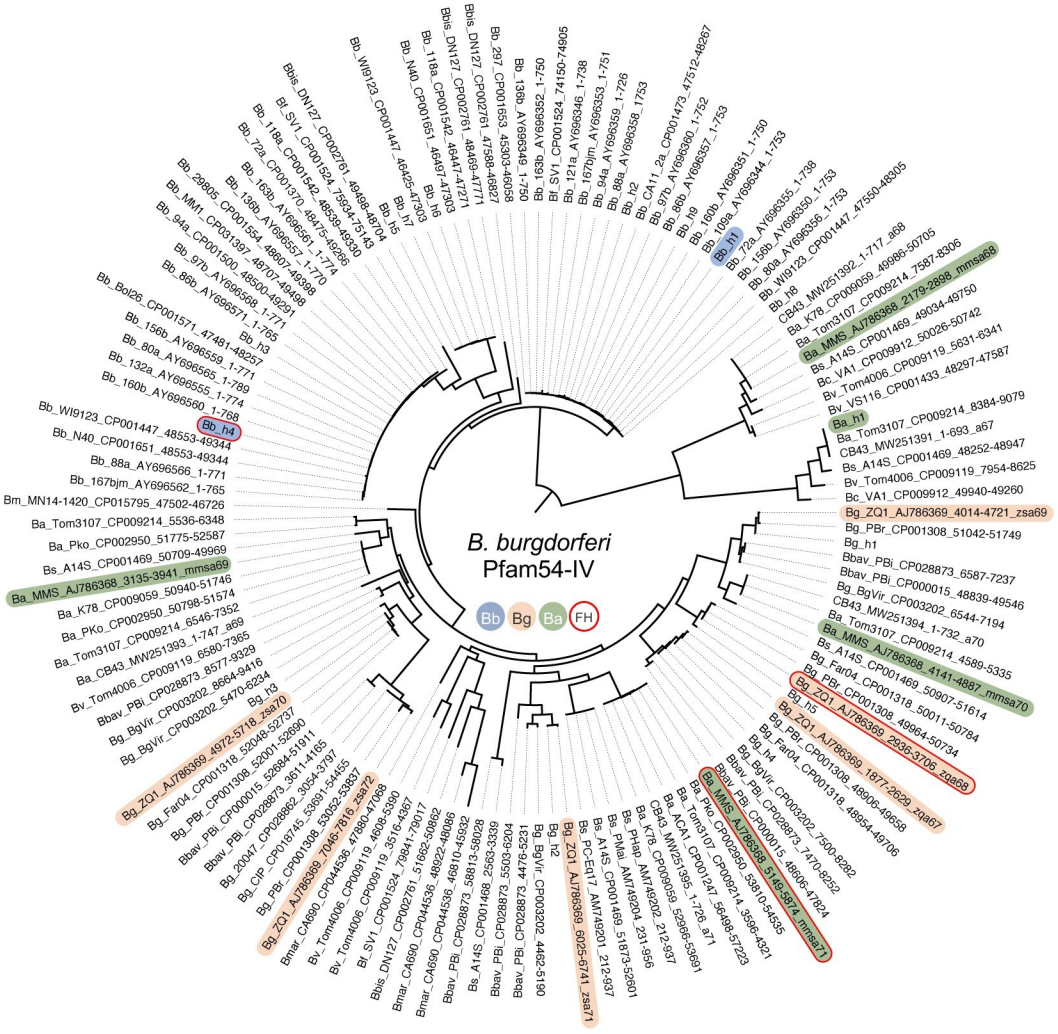

Fig 7. Phylogenetic reconstruction of PFam54-IV proteins from multiple strains of Lyme borreliae genospecies. Maximum likelihood phylogenetic tree using the HIVw+F+R4 amino acid substitution model. Node support was estimated with 1,000 ultrafast bootstrap replicates and 5,000 replicates for the SH-aLRT test. These variants are from indicated strains of *B. burgdorferi* (*Bb*), *B. afzelii* (*Ba*), *B. garinii* (*Bg*), *B. bavariensis* (*Bbav*), *B. valaisiana* (*Bv*), *B. filandensis* (*Bf*), *B. bissettii* (*Bbis*), and *B. mayonii* (*Bm*) available on GenBank. Colors denote Pfam54-IV variants of *B. burgdorferi* strain B31 (blue), *B. garinii* strain ZQ1 (orange), and *B. afzelii* strain MMS (green); the red contour line indicates the variants of Pfam54-IV with mouse and/or quail factor H-binding activity, CspA.

https://doi.org/10.1371/journal.ppat.1009801.g007

support (Bayesian posterior probabilities (PP) of 0.81 at $CspA_{B31}$ and $CspA_{MMS}$ nodes and 0.86 at $CspA_{MMS}$ and $CspA_{ZQ1}$ nodes) (Fig 6D). Similar branching patterns were seen when phylogenetic relationships were estimated among homologs encoding PFam54-IV available on GenBank from *B. burgdorferi*, *B. afzelii*, and *B. garinii* and other Lyme borreliae genospecies with species forming paraphyletic assemblages (Fig 7). We then tested the plausibility of this evolutionary scenario by placing CspA variants in the same clades, grouped by FH-binding functions (Fig 8A, left) or by grouping PFam54-IV variants from the same genospecies together (Fig 8A, right). The sequence data did not support either alternative evolutionary scenarios based on phylogenetic tree topology testing (Fig 8B), in favor of the convergent evolution scenario (better tree log-likelihood value, P = 1.0). Further, the supported phylogeny raises the possibility that CspA-mediated FH-binding activities arose from 1) a common

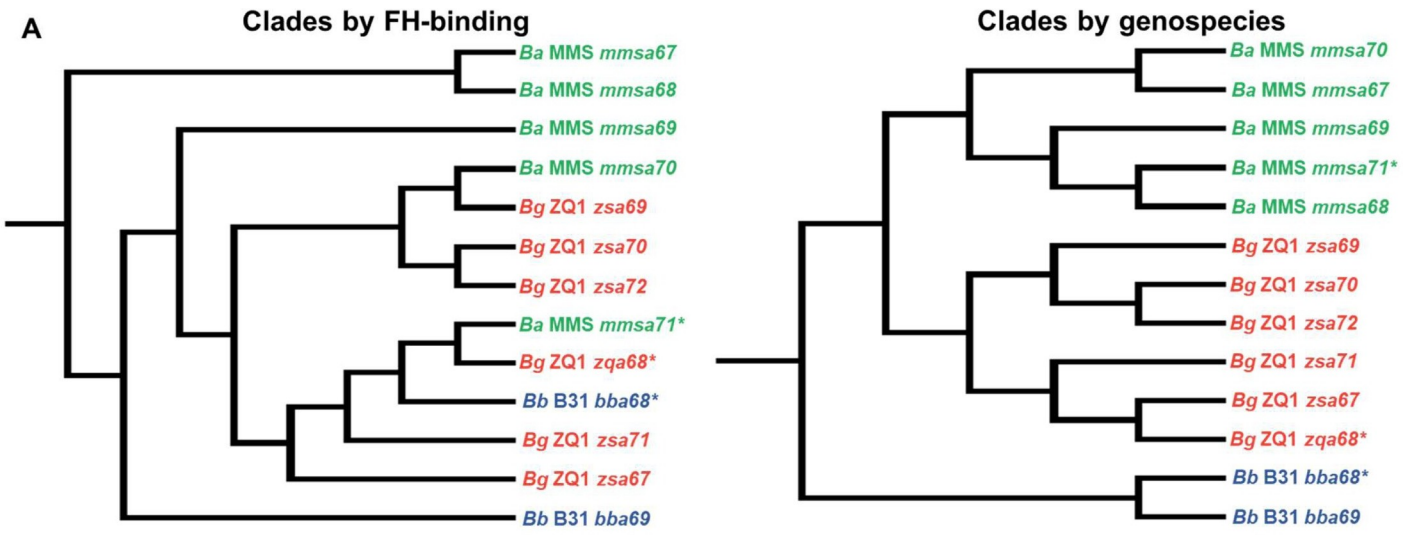

B

Phylogeny forming clades by	logL	bp-RELL	p-KH	p-SH	c-ELW	p-AU
Convergent evolution	-7669.526515	1	1	1	1	1
FH-binding activity	-7814.374806	0	0	0	1.81×10^{-36}	4.95×10^{-6}
Genospecies	-7761.994918	0	0	2×10^{-4}	1.45×10^{-15}	1.56×10^{-4}

Fig 8. Competing evolutionary scenario evaluation of PFam54-IV gene divergence rejects alternative tree topologies of PFam54-IV proteins forming clades by FH-binding activity or spirochete genospecies. (A) Phylogenetic scenarios showing a single emergence of FH-binding or PFam54-IV genes forming clades by genospecies. **(B)** Log-likelihood value for each tree (logL), RELL bootstrap proportion (bp-RELL; 1.0 is full support for that tree), Kishino-Hasegawa test, Shimodaira-Hasegawa test, Expected Likelihood Weights (c-ELW; 1.0 is full support for that tree), and the Approximately Unbiased test (p-AU). Significant p-values indicate comparisons where the best-known ML tree explains the sequence data better than the alternative scenario.

https://doi.org/10.1371/journal.ppat.1009801.g008

FH-binding ancestor or 2) the convergent evolution of PFam54-IV (Fig 6D). However, our results from maximum likelihood and parsimony-based ancestral state reconstruction methods, rejected the FH-binding ancestor scenario (Fig 6D), indicating that the allelically-variable, host-specific FH-binding activity of CspA is a result of convergent evolution within PFam54-IV. Based on a chromosome mutation rate estimated in a previous study [34], this evolutionary event likely occurred approximately 15,000–55,000 years before present, coinciding with the end of the last glacial maximum (Fig 6D).

Discussion

Frequent interactions of pathogens with one or a few hosts may drive them to adapt and become specialized in such host(s), thus maximizing fitness [4,35]. However, the fact that generalists are present in nature suggests that broad host ranges can also confer fitness advantages [4,35]. For vector-borne pathogens, the process leading to host tropism can be driven by host-derived components (i.e. immune molecules or nutrients) either in the hosts or acquired by vectors [4]. The molecular determinants and evolutionary mechanisms by which pathogens specialize or generalize to be associated with hosts are largely unclear. Reflected by the variable hosts carrying different spirochete genospecies transmitted through *Ixodes* ticks, the Lyme disease bacterium is a well-suited model to study host tropism [9,10]. One long-held concept that

have not been definitively tested is that evading host complement immune responses by spirochetes determines Lyme borreliae host tropism [36]. A hurdle for such an investigation is the inability to easily maintain non-mammalian hosts, such as birds, in laboratory and/or persistently infect them [37–47]. Though some wild-birds have been brought into laboratories to study spirochete infectivity [37–47], molecular mechanisms have not been elucidated because of the lack of avian-specific reagents. We and others have used *Coturnix* quail as avian Lyme disease model as this species was found to be fed on by *Ixodes* ticks [48,49] and can sustain detectable spirochete burdens for more than eight weeks [26,27]. In this study, we allowed ticks carrying spirochetes to feed on quail, similar to previous work performed in this species and other domestic aves [50–52]. We found that *B. garinii* ZQ1 and *B. burgdorferi* B31-5A4 survive in fed ticks and are transmitted to quail whereas *B. afzelii* CB43 did not. These results demonstrate that the genospecies variation of spirochete transmissibility to birds, in agreement with prior studies (reviewed in [9]), supporting the use of quail as an avian host representative. In contrast, when nymph feeding was performed on wild-type mice, *B. afzelii* CB43 and *B. burgdorferi* B31-5A4 survived in fed ticks and migrated to these animals while *B. garinii* ZQ1 did not. All three species survived in fed ticks and were transmitted to complement-deficient quail or mice. In support of previous *in vitro* evidence [36,53], this study establishes complement evasion by spirochetes as a driver of Lyme borreliae host tropism. As complement is enriched in vertebrate blood, our findings raise a possibility that spirochetes must evade host complement specifically in tick blood meals.

Tick feeding on live animals used in our study may introduce confounding factors of blood meal-independent, complement-mediated clearance [54]. To address this potential confounder, we use different sources of blood in "artificial feeding chambers" without the involvement of animals. This chamber assay allows us to demonstrate that spirochete evasion to complement in tick blood meals dictates Lyme borreliae host tropism [29]. Nonetheless, it should be noted that heparin as an anti-coagulant required to be used in the blood derived from this feeding chamber assay was reported to impact the complement activation [55–57]. Thus, such a caveat emphasizes the importance of considering the combined evidence from both feeding chamber assays and tick infection animal models.

A potential limitation of the experimental design is that we used *I. scapularis* ticks for all experiments. *B. afzelii* and *B. garinii* are not endemic to North America where *I. scapularis* are commonly found, and have been only isolated from other *Ixodes* ticks (i.e. *I. ricinus* and *I. persulcatus*) in the field. *B. burgdorferi* is the only Lyme borreliae genospecies in this study that is circulated in *I. scapularis* in nature [5]. Specifically, vector competence to a particular pathogen is determined by not only pathogen persistence in molting ticks and the following tick-to-host transmission but also the levels of initial acquisition for a pathogen acquired by uninfected ticks, which was not measured in this study. Thus, utilizing *I. scapularis* as a vector representative may not completely address the role of vector competence in impacting host tropism of spirochetes [58–59]. However, using a single tick species carrying each of the tested spirochete species allows for attribution of the observations solely to host and/or pathogen determinants, the emphasis of this study. Additionally, *I. scapularis* ticks were shown in laboratory infections to acquire and transmit *B. burgdorferi*, *B. afzelii*, and *B. garinii* at similar levels [60–61], suggesting the feasibility to use this tick in representing the *Ixodes* vectors of Lyme disease. Additionally, Lyme borreliae-infected mice have been frequently used to generate nymphs harboring spirochetes through blood feeding by naïve larvae [62]. However, rearing nymphs carrying similar burdens of each spirochete species in this fashion is difficult because wild-type mice do not maintain equal loads of these spirochetes [63–64]. Using complement-deficient mice ($C3^{-/-}$ mice), we found similar burdens of *B. burgdorferi* B31-5A4, *B. afzelii* CB43, and *B. garinii* ZQ1 in fed larvae, post-molting flat nymphs, and the tissues derived from spirochete-infected mice.

Furthermore, it should be noted that C3 not only plays a role as a complement component to confer complement activation but also cross-talks with adaptive immune responses [65], raising the possibility of the adaptive immune response as a confounding factor to influence transmissibility. However, the infection stage tested in this work is very early (7 days post tick feeding), suggesting that this possibility is unlikely. Taken together, our results provide a strategy to overcome the difficulty in tick-rearing and infection, and support the concept that complement controls the spirochete infectivity during infection [21,63,66].

Both *Ixodes* ticks and Lyme borreliae produce complement-inactivating proteins to facilitate feeding and pathogen transmission [8,67–69]. Documented by the fact that many Lyme borreliae proteins are polymorphic, one attractive hypothesis is that polymorphisms in these proteins contribute to host tropism. Regrettably, using wild-type spirochete strains may not delineate the contribution of each of these proteins because these spirochetes have been known to generate multiple polymorphic complement-inactivating proteins [22,70–73]. Thus, identical spirochete background strains have been used to express genes or alleles (also known as "isogenic strains") to define bacterial determinants of particular phenotypes [21,74,75]. We have previously shown that isogenic strains in a *cspA*-deficient background producing CspA from *B. burgdorferi* B31 or *B. afzelii* PKo, but not *B. garinii* ZQ1, promote tick-to-mouse transmission. The ability of ticks to transmit Lyme borreliae is contingent on the ability of the spirochete to survive in fed ticks, consistent with the phenotypes observed using wild-type genospecies [21]. Such differential transmissibility depends on the ability of CspA to bind to mammal FH in the presence of mouse complement, leading to the possibility that allelically-variable, CspA-mediated FH-binding activity dictates host tropism [21,24,25]. Nonetheless, that concept requires identification of the animals that are susceptible to Lyme borreliae that express ZQ1-derived CspA. In agreement with our previous work showing CspA from ZQ1 and B31 but not PKo binds to quail FH [21], we found the ZQ1- and B31- (but not PKo-) derived CspA facilitates tick-to-quail transmission of spirochetes. We further showed that such an allele-dependent, quail-specific transmission is determined by the presence of quail complement and the ability of CspA to bind to this species' FH. Our results using feeding chambers, isogenic bacterial strains and complement-intact or -deficient human or quail blood indicated that CspA is a determinant of Lyme borreliae host tropism by promoting host-specific, FH-binding-dependent complement evasion in tick blood meals. Note that this study does not rule out the possibility of other anti-complement proteins in promoting host-specific infectivity as *cspA* is downregulated after spirochete transmission to vertebrate animals [21,23]. Instead, these results demonstrated the role of CspA to facilitate spirochete in overcoming the initial barrier of tick-to-host transmission in determining host tropism.

CspA, like other Pfam54-IV proteins, experienced numerous duplication and loss events, resulting in moderate sequence identity (~40 to 80%) among variants in this protein family [32,33,76]. This is suggestive of rapid evolution, and potential neofunctionalization [32,33,77], supported by some important functions (e.g. complement evasion, cell adhesion, plasminogen binding, and tissue colonization) identified for CspA and other Pfam54 proteins [21,78–81]. However, the moderate sequence similarity from a limited number of strains in those studies renders the establishment of 1:1 orthology relationships difficult across Pfam54-IV [32,33], thus impacting the examination of evolutionary mechanisms giving rise to those functions. By comparing the sequences that encode PFam54-IV from different strains within each genospecies, we found a wide range of sequence diversity. These results allow us to define these highly similar sequences as paralogs. These findings also suggest that the phenotypes conferred by one Pfam54-IV protein (e.g. host-specific FH-binding activity/transmissibility) are likely shared by its orthologs from different strains within the same genospecies [82]. Furthermore, we observed notably divergence (pairwise identity <79%) between the genes encoding

Pfam54-IV among different spirochete genospecies, indicating that at least some genospecies-specific polymorphisms have reached fixation. These results, combined with the fact that CspA variants confer variable complement evasion and host tropism [21,24,25], are in line with the findings of allelically-variable phenotypes in other Lyme borreliae polymorphic proteins [72,74,75]. Furthermore, these data suggest that any unidentified functions of CspA or other Pfam54-IV may vary among the strains from different genospecies.

Some phenotypes are shared among multiple Pfam54-IV proteins from the same Lyme borreliae genospecies (e.g. C7 and C9 binding-mediated complement evasion by Bga66 and Bga71 from *B. bavariensis*) [78]. This finding raises the possibility that FH-binding is a common feature for non-CspA Pfam54-IV proteins within the same genospecies. However, our finding showing no detectable mouse or quail FH-binding to non-CspA Pfam54-IV indicates that the FH-binding activity is unique to CspA, in agreement with the results of human FH-binding activity of Pfam54-IV [24]. Further, our data from phylogenetic reconstructions rejected the possibility of functional cladding of CspA or a common FH-binding ancestor, but supported convergent evolution as the mechanism leading to such an allelically variable, CspA-mediated FH-binding activity [83]. With the fact that such an activity dictates Lyme borreliae host tropism, allelically variable CspA-mediated FH-binding activity would effectively isolate different populations of Lyme borreliae in their respective hosts in nature, resulting in adaptive radiation of spirochetes. An intriguing question is whether the emergence of such host-specific FH binding is concurrent with allopatric ecological speciation of the Lyme borreliae whereby host switching events isolated groups of spirochetes. This would lead the spirochetes to evolve the ability, such as the host-specific FH binding activity of CspA, in response to disparate host environments and leading to adaptations [84–90]. However, the phylogenetic reconstruction of Pfam54-IV suggests that CspA of *B. burgdorferi* evolved approximately 15,000 to 55,000 years before present (BP), while the earliest common ancestor of *B. burgdorferi* in North America was dated at ~60,000 years BP [34]. Thus, the emergence of the CspA variants likely occurred after ancient Lyme borreliae speciation. Our timeline of CspA emergence coincides with the latter half of the last glacial maximum in North America and Europe, which was a period of major climactic change [91–92]. A plausible explanation is that this drastically changing environment resulted in novel selective pressures, such as changes to host body condition and immune response, or host and vector availability and ranges [93–95]. In response to such changes, the spirochetes may have evolved new strategies to be maintained in the enzootic cycle, such as allelically variable, CspA-mediated FH-binding activity. Using the Lyme disease bacterium as a model, this work is a pioneering study defining the mechanisms that dictate host tropism of pathogens, identifying the molecular determinants, and elucidating the evolutionary drivers of such host-pathogen associations. These findings will provide significant impacts into the origin of a vector-borne enzootic cycle and establish the groundwork for future studies to investigate the mechanisms in shaping host tropism.

Materials and methods

Ethics statement

All mouse and quail experiments were performed in strict accordance with all provisions of the Animal Welfare Act, the Guide for the Care and Use of Laboratory Animals, and the PHS Policy on Humane Care and Use of Laboratory Animals. The protocol was approved by the Institutional Animal Care and Use Committee (IACUC) of Wadsworth Center, New York State Department of Health (Protocol docket number 19–451) and Columbia University (Protocol docket number AC-AAAO4551). All efforts were made to minimize animal suffering.

Mouse, quail, tick, bacterial strains, OmCI, and FH

BALB/c mice were purchased from Taconic (Hudson, NY). $C3^{-/-}$ mice in BALB/c background were generated from the $C3^{-/-}$(C57BL/6) purchased from Jackson Laboratory (Bar Harbor, ME) as described in our previous study [21]. *P. leucopus* mice were ordered from *Peromyscu*s genetic stock center at University of South Carolina (Columbia, SC). *Coturnix* quail was purchased from Cavendish Game Birds Farm (Springfield, VT). *Ixodes scapularis* tick larvae were purchased from National Tick Research and Education Center, Oklahoma State University (Stillwater, OK) or obtained from BEI Resources (Manassas, VA). Lyme borreliae-infected nymphs were generated as described in the section "Generation of ticks carrying Lyme borreliae." The *Borrelia* and *Escherichia coli* strains used in this study are described in S2 Table. *E. coli* strains DH5α, M15, and derivatives were grown in Luria-Bertani (BD Bioscience) broth or agar, supplemented with kanamycin (50μg/ml), ampicillin (100μg/ml), or no antibiotics as appropriate. All *B. burgdorferi*, *B. afzelii*, and *B. garinii* strains were grown in BSK-II completed medium supplemented with kanamycin (200μg/mL), streptomycin (50μg/mL), gentamicin (50μg/mL), or no antibiotics (see S2 Table). Mouse FH was purchased from MyBiosource. Quail FH and recombinant OmCI proteins were generated as described previously [21,26,28].

Mouse infection using needle inoculation

Four-week-old female BALB/c or $C3^{-/-}$ mice in BALB/c background were used for experiments involved in needle infection of Lyme borreliae strains. Mice were infected by intradermal injection as previously described [75] with 10^6 of *B. afzelii* CB43, *B. garinii* ZQ1, or *B. burgdorferi* B31-5A4. The plasmid profile of the strain B31-5A4 was verified prior to infection as described to ensure the stability of the vector and no loss of plasmids [96–97]. As the information of genome is not available for plasmid profiling, the strains CB43 and ZQ1 used in this study were less than ten passages. Mice were sacrificed at 21 days post-infection, the inoculation site of the skin, the ankle joints, ears, and bladder were collected to quantitatively evaluate levels of colonization during infection as described in the section "Determination of Lyme borreliae burdens in infected ticks, tissues and blood samples.".

Generation of ticks carrying Lyme borreliae

The procedure of the tick infection has been described previously [21,98]. Basically, four-week-old male and female $C3^{-/-}$ mice in BALB/c background were infected with 10^6 of *B. afzelii* CB43, *B. garinii* ZQ1, or *B. burgdorferi* B31-5A4, B31-5A15, B31-5A4NP1Δ*cspA* harboring a vector or this *cspA* mutant strain producing $CspA_{B31}$, $CspA_{PKo}$, $CspA_{ZQ1}$, or $CspA_{B31}$L246D by intradermal injection as described above. The ear punches from those mice were collected at 13 days post infection, and DNA was extracted to perform qPCR using *Borrelia* 16S rRNA primers as previously described [26] (S3 Table) to confirm the infection (See section "Determination of Lyme borreliae burdens in infected ticks, tissues and blood samples."). At 14 days post infection, the uninfected larvae were allowed to feed to repletion on those spirochete-infected mice as described previously [21,98]. Approximately 100 to 200 larvae were allowed to feed on each mouse. The engorged larvae were collected and allowed to molt into nymphs in a desiccator at room temperature and 95% relative humidity in a room with light dark control (light to dark, 16:8 h). [21,96].

Serum resistance assays

Coturnix quail were subcutaneously injected with OmCI (1 mg/kg of quail) or PBS buffer, and the sera were collected at 6, 24, 48, 72, and 96 h post injection. A serum sensitive, high passaged

B. burgdorferi strain B313 was cultivated to mid-log phase, followed by being diluted to a final concentration of 5×10^6 bacteria/ml in BSKII medium without rabbit serum. These bacteria were then incubated with each of these quail serum samples (final concentration: 40% of serum). We also included the bacteria mixed with heat inactivated serum samples, which have been incubated at 56˚C for 2h prior to being mixed with spirochetes. An aliquot was taken from each reaction at 0 and 4h post injection to determine the number of motile bacteria under a Nikon Eclipse E600 darkfield microscope, as previously described [21]. The survival percentage for those motile spirochetes was calculated using the number of mobile spirochetes at 4h post incubation normalized to that at the very beginning of incubation with serum.

Mouse, quail, and *P. leucopus* infection by ticks

The flat nymphs were placed in a chamber on four- to six-week old male and female BALB/c or $C3^{-/-}$ mice in BALB/c background, and the engorged nymphs were collected from the chambers at seven days post nymph feeding as described [99]. For ticks feeding on quail, the feathers located on the back of quail's neck were plucked to expose approximately 2–3 cm^2 of skin, close to the back of its head. 1.2ml screw-top cryo-microcentrifuge vials (ThermoFisher Scientific) were cut to be used as mini chambers. The top of the caps from the chambers was pierced with a 25-gauge needle to create air holes, and sand papers were used to smooth any sharp edges along the cut surface edge of these chambers. Vetbond Tissue Adhesive (3M) was used to attach the chambers onto the exposed quail skin followed by manually restraining quail while the surgical glue dries (1-2min). Ten nymphs were placed into the chambers on mice or quail, which those ticks to feed on. For OmCI-treated quail, the quail were subcutaneously injected with OmCI (1mg/kg of quail) a day prior to the nymph feeding. The engorged nymphs were obtained from the chambers. The mice and quail were placed into a small cage, which then placed above the moat in a larger cage (for mice) or plastic bin (for quail). Ticks feeding on *Peromyscus leucopus* mice have been described previously [100–101]. Ten nymphs were placed in the ears of each mouse, five nymphs per ear and were allowed to feed until repletion. *P. leucopus* mice were separately placed in water cages which consisted of the cage being filled with approximately 2.5cm of water along the bottom, a wire rack to keep the mouse out of the water, and then being placed in a larger hamster cage with water to prevent ticks from escaping. The engorged nymphs were recovered from the water cage beginning five days post nymph feeding. Blood and tick placement site from quail, mice, and *P. leucopus* mice were collected at seven days post nymph feeding.

Feeding chamber assays by ticks

Artificial feeding chambers were prepared as described in our previous study [21]. In short, the silicone rubber-saturated rayon membrane was generated as described [21], with the exception of adhering fiberglass mesh (3-mm pore; Lowe's Inc.) to the membrane before attaching it to the rest of the chamber. Such membrane was attached to one side of a 2-cm length of polycarbonate tubing (hereafter called the chamber; inner diameter: 2.5 cm; outer diameter: 3.2 cm; (Amazon Inc.), as described, with the exception of using a rubber band to hold the chamber in place instead of a rubber O-ring [21]. Feeding stimuli including hair and hair extract from white-tailed deer (*Odocoileus virginianus*) and a plastic tile spacer (Lowe's Inc.) were added as described with the exception of using 3 stainless steel bearings (Amazon Inc.) instead of a nickel coin [21]. *I. scapularis* nymphs carrying *B. burgdorferi* B31-5A4, *B. afzelii* CB43, *B. garinii* ZQ1; or *B. burgdorferi* B31-5A4, B31-5A15, B31-5A4NP1Δ*cspA* harboring a vector or this *cspA* mutant strain producing $CspA_{B31}$, $CspA_{PKo}$, $CspA_{ZQ1}$, or $CspA_{B31}$L246D were then added onto the chamber (5 to 8 ticks/chamber). Chamber feedings

were carried out as previously described using human (BioIVT, Westbury, NY) or quail blood (Canola Poultry Market, Brooklyn, NY) (Fig 2A), which were treated with heparin (final concentration 75 U/ml for quail blood) and pre-warmed at 37˚C for 45 min. Chambers in blood were placed in a sealed Styrofoam cooler with wet paper towels to maintain humidity at approximately 87 to 95% in an incubator at 37˚C. Depending on the experiments, blood was treated with CVF (ComTech) or OmCI to a final concentration of 17 μg/ml. Blood was changed daily and was collected along with ticks only after 5 days of feeding. SYBR-based qPCR was used to determine bacterial burdens in the ticks and blood using *Borrelia* 16S rRNA gene primers (S3 Table).

Determination of Lyme borreliae burdens in infected ticks, tissues and blood samples

The ticks fed on quail, mice, *P. leucopus* mice, or feeding chambers were homogenized by hand in a 1.5 ml Eppendorf tube (Eppendorf) with a plastic pestle (ThermoFisher Scientific). The DNA from tissues or blood or homogenized ticks was extracted using the EZ-10 Genomic DNA kit (Biobasic). The quantity and quality of DNA was assessed using a Nanodrop 1000 UV/Vis spectrophotometer (ThermoFisher Scientific). The 280:260 ratio was between 1.75 and 1.85, indicating the lack of contaminating RNA or proteins. qPCR was then performed to quantitate bacterial loads. Spirochete genomic equivalents were calculated using an ABI 7500 Real-Time PCR System (ThermoFisher Scientific) in conjunction with PowerUp SYBR Green Master Mix (ThermoFisher Scientific), based on amplification of the Lyme borreliae 16S rRNA gene using primers 16SrRNAfp and 16SrRNArp (S3 Table), as described previously [23,75]. Cycling parameters for SYBR green-based reactions were 50˚C for 2min, 95˚C for 10min, and 45 cycles of 95˚C for 15s, 55˚C for 30s, and 60˚C for 1min. The number of 16S rRNA copies was calculated by establishing a threshold cycle (Cq) standard curve of a known number of 16S rRNA gene extracted from *B. burgdorferi* strain B31-5A4, then comparing the Cq values of the experimental samples.

Sequence analysis of PFam54-IV

Nucleotide sequences of the PFam54-IV genes, including *bba68* ($cspA_{B31}$), and *bba69* from *B. burgdorferi* B31 (AE000790), *pkoa0062*, *pkoa0063*, *pkoa0064*, *pkoa0065*, *pkoa0066*, and *pkoa0067* ($cspA_{PKo}$), from *B. afzelii* PKo (CP002950), and *zqa67*, *zqa68* ($cspA_{ZQ1}$), *zsa69*, *zsa70*, *zsa71*, and *zsa72* from *B. garinii* ZQ1 (AJ786369), were used as queries against the NCBI GenBank nr database using BLASTN [102]. Sequences from organisms other than *B. burgdorferi*, *B. afzelii*, and *B. garinii* and duplicate sequences were discarded. The remaining sequences were then adjusted to include the full open reading frames with removal of any sequences containing premature stop codons. Sequences were grouped by species, and the sequences of the genes encoding the third and fifth clade of PFam54 (PFam54-III and Pfam54-V, respectively) from *B. burgdorferi* B31, *B. afzelii* PKo, and *B. garinii* ZQ1 were added to the sequence set (GenBank accession codes are found on S5–S7 Figs). Codon alignments were generated using T-Coffee on the TranslatorX webserver [103–104], followed by calculation of pairwise sequence identity in Clustal Omega [105]. Only Pfam54-IV best hits were kept. The remaining sequences were then realigned by codon and pairwise identity was calculated as above. (S5–S7 Figs).

Generation of recombinant PFam54 proteins

The pQE30Xa vectors encoding the open reading frames lacking the putative signal sequences of *bba68* ($cspA_{B31}$), *bba69* from *B. burgdorferi* strain B31-5A4, *mmsa67*, *mmsa68*, *mmsa69*, or

mmsa70, and *mmsa71* ($cspA_{MMS}$) from *B. afzelii* strain MMS, or *zqa67*, *zqa68* ($cspA_{ZQ1}$), *zsa69*, *zsa70*, *zsa71*, or *zsa72* from *B. garinii* strain ZQ1 were obtained previously to generate recombinant histidine-tagged proteins [24]. The plasmids were transformed into *E. coli* strain M15, and the plasmid inserts were sequenced using Sanger sequencing on an ABI 3730xl DNA Analyzer (ThermoFisher Scientific) at the NYSDOH Wadsworth Center ATGC Core Facility. The resulting M15 derived strains were used to produce respective recombinant PFam54-IV (S2 Table). The histidine-tagged PFam54-IV were produced and purified by nickel affinity chromatography with Ni-NTA agarose according to the manufacturer's instructions (Qiagen).

FH binding assay by qualitative ELISA

Qualitative ELISA for FH binding by PFam54-IV was performed as described [21,106]. One microgram of BSA (negative control; Sigma-Aldrich) or FH from mouse or quail was coated onto microtiter plate wells by incubating the plate for overnight at 4˚C. Then, 100 μl 2 μM of histidine-tagged DbpA from *B. burgdorferi* strain B31 (negative control) [107] or each of the PFam54-IV was added to the wells. Mouse anti-histidine tag 1:200× (Sigma-Aldrich) and HRP-conjugated goat anti-mouse IgG 1:1,000× (Seracare Life Sciences) were used as primary and secondary antibodies, respectively, to detect the binding of histidine-tagged proteins. The plates were washed three times with PBST (0.05% Tween 20 in PBS), and 100 μl of tetramethyl benzidine (TMB) solution (ThermoFisher Scientific) was added to each well and incubated for 5 min. The reaction was stopped by adding 100μl of 0.5% hydrosulfuric acid to each well. Plates were read at 405nm using a Tecan Sunrise Microplate reader at 5 min post incubation (Tecan Life Science).

Phylogenetic reconstruction

The PFam54-IV codon alignment from *B. burgdorferi* B31, *B. afzelii* MMS, and *B. garinii* ZQ1 was used to estimate a Bayesian phylogenetic tree in BEAST v1.8.4 with a relaxed lognormal clock, an estimated mutation rate of 4.75×10^{-6} substitutions/site/year and a coalescent Bayesian skyline model [34,108]. A Markov chain Monte Carlo chain length of 10,000,000 steps was used with a 100,000-step thinning, resulting in effective sample sizes greater than 200, an indication of an adequate chain mixing. The resulting maximum clade credibility tree was visualized in FigTree v1.4.4 [109]. We evaluated alternative, competing evolutionary scenarios for PFam54-IV based on species-specific divergence, or clustering by FH-binding activity shown in Fig 8A [110]. A battery of statistical phylogenetic tests was deployed in IQ-TREE (Kishino-Hasegawa, Shimodaira-Hasegawa, Expected Likelihood Weights, and Approximately Unbiased tests)[111–114]. The more extensive dataset was created by aligning all relevant PFam54-IV protein sequences using M-Coffee [115] (http://www.tcoffee.org) and estimating phylogenetic relationships using maximum likelihood in IQ-TREE v1.6.14 [116]. The best fit substitution model HIVw+F+R4 among 344 candidate models, including empirical amino acid frequencies and among-site rate heterogeneity modeling, was selected based on the Bayesian Information Criterion (BIC-weight = 0.9583) using the ModelFinder [117] feature in IQ-TREE. Node robustness was assessed with 1000 ultrafast bootstrap replicates [118] and the SH-aLRT test with 5000 replicates [119].

Statistical analysis

Significant differences between samples were assessed using the Mann-Whitney *U* test or the Kruskal-Wallis test with the two-stage step-up method of Benjamini, Krieger, and Yekutieli. A P-value < 0.05 (*) or ($^{\#}$) was considered to be significant [120].

Supporting information

S1 Fig. Lyme borreliae vary in their ability to infect mice via intradermal injection of BALB/c but not C3$^{-/-}$ BALB/c mice. (A to D) BALB/c or **(E to H)** C3$^{-/-}$ BALB/c mice were injected with 10^6 *B. burgdorferi* B31-5A4 ("*Bb* B31-5A4"), *B. garinii* ZQ1 ("*Bg* ZQ1"), or *B. afzelii* CB43 ("*Ba* CB43"). At 21 days post injection ("dpi"), spirochete burdens were determined in the **(A and E)** inoculation site ("Inoc. site"), **(B and F)** ears, **(C and G)** bladder, **(D and H)** ankles. Additionally, uninfected *I. scapularis* larvae were allowed to feed on those C3$^{-/-}$ mice at 14 days post injection ("dpi") to repletion. Spirochete burdens in **(I)** replete larvae, and **(J)** post molting flat nymphs ("flat nymphs") were determined. The tissues from uninfected mice and uninfected nymphs were included as control ("Uninfect."). Shown are the geometric means of bacterial loads ± 95% confidence interval of bacterial burdens from 6 replete larvae, flat nymphs or tissues from 5 BALB/c mice or indicated numbers of C3$^{-/-}$ BALB/c mice (9 *Bb* B31-5A4-infected inoculation sites and ears, 6 *Bg* ZQ1-infected inoculation sites and ears, or 5 all other tissues). Significant differences ($p < 0.05$, Kruskal-Wallis test with the two-stage step-up method of Benjamini, Krieger, and Yekutieli) in the spirochete burdens relative to uninfected ticks or tissues (*) are indicated.
(TIF)

S2 Fig. The complement of quail inoculated with OmCI is inactivated. *Coturnix* quail were subcutaneously injected with OmCI (1 mg/kg of quail) or PBS buffer. Untreated (black bars) or heat-treated (white bars) of sera collected from these quail at indicated time points after inoculation were incubated with a serum-sensitive, highly passaged *B. burgdorferi* strain B313 for 0-h and 4-h with a final concentration of 40%. The number of motile spirochetes was assessed through microscopy. The survival percentage of the spirochetes was calculated using the number of mobile spirochetes at 4 h post incubation normalized to that at 0 h of incubation with serum. Each bar represents the mean of three independent determinations ± SEM from sera from five quail per group. Significant differences ($p < 0.05$, Kruskal-Wallis test with the two-stage step-up method of Benjamini, Krieger, and Yekutieli) in the percentage survival of spirochetes incubated with untreated sera from OmCI-inoculated quail, compared to that in heat-inactivated sera from those quail (*).
(TIF)

S3 Fig. Protein sequence alignment of CspA variants from *B. afzelii* CB43, PKo, and MMS and the synteny from PFam54-IV proteins of these strains. (A) CspA variants from *B. afzelii* CB43, PKo, and MMS aligned in M-Coffee. Blue shading indicates complete sequence conservation. **(B)** Synteny of Pfam54-IV genes. Colors indicate one-to-one orthologs. Locus *pkoa0066* is only found in strain PKo. Scale bar denotes 500 bp.
(TIF)

S4 Fig. CspA variants confer differential transmissibility from nymphs to *P. leucopus* mice. *Ixodes scapularis* nymphs infected by WT *B. burgdorferi* B31-5A15 ("B31-5A15"), *B. burgdorferi* B31-5A4NP1*ΔcspA* transformed with an empty shuttle vector ("Vector"), or this deletion strain producing a mutated variant of CspA from *B. burgdorferi* B31 selectively devoid of FH binding activity ("L246D"), WT *B. burgdorferi* B31 ("B31"), *B. garinii* ZQ1 ("ZQ1"), or *B. afzelii* PKo ("PKo") were allowed to feed to repletion on *P. leucopus* mice. Uninfected nymphs and *P. leucopus* mouse tissues and blood were included as control ("Uninfect."). Fed nymphs were collected upon repletion, and blood and tissues were collected at 7 days post nymph feeding ("dpf"). Spirochete burdens in **(A)** replete nymphs, **(B)** tick bite sites of skin ("Inoc. site"), and **(C)** blood were determined by qPCR. For spirochete burdens in tissue samples, the resulting values were normalized to 100 ng of total DNA. Shown are the geometric means of bacterial loads ± 95% confidence interval of bacterial burdens in tissues from five *P.*

leucopus mice per group or replete nymphs (8 nymphs carrying the strain B31-5A15, 12 nymphs carrying the strain "Vector", 13 nymphs carrying the strain pCspA-B31, 15 nymphs carrying the strain pCspA-PKo, or 13 nymphs carrying the strain pCspA-ZQ1). Significant differences ($p < 0.05$, Kruskal-Wallis test with the two-stage step-up method of Benjamini, Krieger, and Yekutieli) in the spirochete burdens relative to uninfected ticks or *P. leucopus* mouse tissues or blood are indicated (*).
(TIF)

S5 Fig. Genetic divergence of Pfam54-IV alleles from *B. burgdorferi*. Nucleotide sequences encoding PFam54-IV proteins from *B. burgdorferi* B31 were used as queries to mine NCBI GenBank for orthologs. **(inset)** Frequency distribution of pairwise genetic distances. The pairwise identity numbers are coded by color gradually from identical (100% pairwise identity; green) to divergent sequences (70% pairwise identity; red). The clear break in the frequency distribution separates highly similar (> 95% pairwise identity) from moderately divergent comparisons (< 80%). The Pfam54-IV ortholog from a particular *B. burgdorferi* strain with > 95% identity to $cspA_{B31}$ was defined as the *cspA* ortholog in that strain.
(TIF)

S6 Fig. Genetic divergence of Pfam54-IV alleles from *B. afzelii*. Nucleotide sequences encoding PFam54-IV proteins from *B. afzelii* PKo were used as queries to mine NCBI GenBank for orthologs. **(inset)** Frequency distribution of pairwise genetic distances. The pairwise identity numbers are coded by color gradually from identical (100% pairwise identity; green) to divergent sequences (40% pairwise identity; red). The clear break in the frequency distribution separates highly similar (> 98% pairwise identity) from moderately divergent comparisons (< 80%). The Pfam54-IV ortholog from a particular *B. afzelii* strain with > 98% identity to $cspA_{B31}$ was defined as the *cspA* ortholog in that strain.
(TIF)

S7 Fig. Genetic divergence of Pfam54-IV alleles from *B. garinii*. Nucleotide sequences encoding PFam54-IV proteins from *B. garinii* ZQ1 were used as queries to mine NCBI GenBank for orthologs. **(inset)** Frequency distribution of pairwise genetic distances. The pairwise identity numbers are coded by color gradually from identical (100% pairwise identity; green) to divergent sequences (65% pairwise identity; red). The clear break in the frequency distribution separates highly similar (> 93% pairwise identity) from moderately divergent comparisons (< 80%). The Pfam54-IV ortholog from a particular *B. garinii* strain with > 93% identity to $cspA_{B31}$ was defined as the CspA ortholog in that strain.
(TIF)

S1 Table. Host-specific transmissibility and FH-binding activity of *B. burgdorferi*, *B. afzelii*, and *B. garinii*, and their derived PFam54-IV proteins.
(DOCX)

S2 Table. *Borrelia* sp. strains and plasmids used in this study.
(DOCX)

S3 Table. PCR primers used in this study.
(DOCX)

Acknowledgments

We thank Frank Blaisdell, and Dierdre Torrisi from the Wadsworth vet sciences facility and Ashley Marcinkiewicz and Patricia Lederman for animal husbandry, Levi Poirier and

Ing-Nang Wang for assistance with Sanger sequencing, Ashley Marcinkiewicz for critical reading of the manuscript, Patricia Rosa for sharing the unpublished observation of *B. afzelii* strain PKo, and Roxie Giradin for assistance with SDS-PAGE. We thank Wadsworth ATGC core for plasmid sequencing, Leslie Eisele of Wadsworth Biochemistry and Immunology Core for HPLC performance, and Karen Chave of the Wadsworth Protein Expression Core for purifying factor H.

Author Contributions

Conceptualization: Thomas M. Hart, Sergios-Orestis Kolokotronis, Yi-Pin Lin.

Data curation: Thomas M. Hart, Alan P. Dupuis, II, Danielle M. Tufts, Maria A. Diuk-Wasser, Sergios-Orestis Kolokotronis, Yi-Pin Lin.

Formal analysis: Thomas M. Hart, Sergios-Orestis Kolokotronis, Yi-Pin Lin.

Funding acquisition: Ryan O. M. Rego, Peter Kraiczy, Laura D. Kramer, Maria A. Diuk-Wasser, Sergios-Orestis Kolokotronis, Yi-Pin Lin.

Investigation: Thomas M. Hart, Alan P. Dupuis, II, Danielle M. Tufts, Simon R. Starkey, Peter Kraiczy, Laura D. Kramer, Maria A. Diuk-Wasser, Sergios-Orestis Kolokotronis, Yi-Pin Lin.

Methodology: Thomas M. Hart, Alan P. Dupuis, II, Danielle M. Tufts, Anna M. Blom, Simon R. Starkey, Peter Kraiczy, Laura D. Kramer, Sergios-Orestis Kolokotronis, Yi-Pin Lin.

Project administration: Laura D. Kramer, Maria A. Diuk-Wasser, Sergios-Orestis Kolokotronis, Yi-Pin Lin.

Resources: Alan P. Dupuis, II, Anna M. Blom, Ryan O. M. Rego, Sanjay Ram, Peter Kraiczy, Sergios-Orestis Kolokotronis, Yi-Pin Lin.

Software: Thomas M. Hart, Sergios-Orestis Kolokotronis, Yi-Pin Lin.

Supervision: Laura D. Kramer, Maria A. Diuk-Wasser, Sergios-Orestis Kolokotronis, Yi-Pin Lin.

Validation: Thomas M. Hart, Sergios-Orestis Kolokotronis, Yi-Pin Lin.

Visualization: Thomas M. Hart, Yi-Pin Lin.

Writing – original draft: Thomas M. Hart, Sergios-Orestis Kolokotronis, Yi-Pin Lin.

Writing – review & editing: Thomas M. Hart, Alan P. Dupuis, II, Danielle M. Tufts, Anna M. Blom, Simon R. Starkey, Ryan O. M. Rego, Sanjay Ram, Peter Kraiczy, Laura D. Kramer, Maria A. Diuk-Wasser, Sergios-Orestis Kolokotronis, Yi-Pin Lin.

References

1. Kilpatrick AM, Altizer S. Disease Ecology. Nature Education Knowledge. 2010; 3(10):55.
2. Killilea ME, Swei A, Lane RS, Briggs CJ, Ostfeld RS. Spatial dynamics of lyme disease: a review. Ecohealth. 2008; 5(2):167–95. https://doi.org/10.1007/s10393-008-0171-3 PMID: 18787920
3. Douam F, Gaska JM, Winer BY, Ding Q, von Schaewen M, Ploss A. Genetic Dissection of the Host Tropism of Human-Tropic Pathogens. Annual review of genetics. 2015; 49:21–45. https://doi.org/10.1146/annurev-genet-112414-054823 PMID: 26407032
4. Kurtenbach K, Hanincova K, Tsao JI, Margos G, Fish D, Ogden NH. Fundamental processes in the evolutionary ecology of Lyme borreliosis. Nature reviews Microbiology. 2006; 4(9):660–9. https://doi.org/10.1038/nrmicro1475 PMID: 16894341

5. Steere AC, Strle F, Wormser GP, Hu LT, Branda JA, Hovius JW, et al. Lyme borreliosis. Nature reviews Disease primers. 2016; 2:16090. https://doi.org/10.1038/nrdp.2016.90 PMID: 27976670

6. Radolf JD, Caimano MJ, Stevenson B, Hu LT. Of ticks, mice and men: understanding the dual-host lifestyle of Lyme disease spirochaetes. Nature reviews Microbiology. 2012; 10(2):87–99. https://doi.org/10.1038/nrmicro2714 PMID: 22230951

7. Brisson D, Drecktrah D, Eggers CH, Samuels DS. Genetics of *Borrelia burgdorferi*. Annual review of genetics. 2012; 46:515–36. https://doi.org/10.1146/annurev-genet-011112-112140 PMID: 22974303

8. Kurokawa C, Lynn GE, Pedra JHF, Pal U, Narasimhan S, Fikrig E. Interactions between *Borrelia burgdorferi* and ticks. Nature reviews Microbiology. 2020; 18(10):587–600. https://doi.org/10.1038/s41579-020-0400-5 PMID: 32651470

9. Tufts DM, Hart TM, Chen GF, Kolokotronis SO, Diuk-Wasser MA, Lin YP. Outer surface protein polymorphisms linked to host-spirochete association in Lyme borreliae. Molecular microbiology. 2019; 111(4): 868–82. https://doi.org/10.1111/mmi.14209 PMID: 30666741

10. Lin YP, Diuk-Wasser MA, Stevenson B, Kraiczy P. Complement Evasion Contributes to Lyme Borreliae-Host Associations. Trends in parasitology. 2020; 36(7):634–45. https://doi.org/10.1016/j.pt.2020.04.011 PMID: 32456964

11. Zhou W, Brisson D. Interactions between host immune response and antigenic variation that control *Borrelia burgdorferi* population dynamics. Microbiology (Reading). 2017; 163(8):1179–88. https://doi.org/10.1099/mic.0.000513 PMID: 28771127

12. Gomez-Chamorro A, Battilotti F, Cayol C, Mappes T, Koskela E, Boulanger N, et al. Susceptibility to infection with *Borrelia afzelii* and TLR2 polymorphism in a wild reservoir host. Scientific reports. 2019; 9(1):6711. https://doi.org/10.1038/s41598-019-43160-3 PMID: 31040326

13. Zipfel PF, Skerka C. Complement regulators and inhibitory proteins. Nature reviews Immunology. 2009; 9(10):729–40. https://doi.org/10.1038/nri2620 PMID: 19730437

14. Blom AM. The role of complement inhibitors beyond controlling inflammation. Journal of internal medicine. 2017; 282(2):116–28. https://doi.org/10.1111/joim.12606 PMID: 28345259

15. Jozsi M, Zipfel PF. Factor H family proteins and human diseases. Trends in immunology. 2008; 29 (8):380–7. https://doi.org/10.1016/j.it.2008.04.008 PMID: 18602340

16. Ermert D, Ram S, Laabei M. The hijackers guide to escaping complement: Lessons learned from pathogens. Molecular immunology. 2019; 114:49–61. https://doi.org/10.1016/j.molimm.2019.07.018 PMID: 31336249

17. Dulipati V, Meri S, Panelius J. Complement evasion strategies of *Borrelia burgdorferi* sensu lato. FEBS letters. 2020; 594(16):2645–56. https://doi.org/10.1002/1873-3468.13894 PMID: 32748966

18. Skare JT, Garcia BL. Complement Evasion by Lyme Disease Spirochetes. Trends in microbiology. 2020; 28(11): 889–899. https://doi.org/10.1016/j.tim.2020.05.004 PMID: 32482556

19. Lin YP, Frye AM, Nowak TA, Kraiczy P. New Insights Into CRASP-Mediated Complement Evasion in the Lyme Disease Enzootic Cycle. Frontiers in cellular and infection microbiology. 2020; 10:1. https://doi.org/10.3389/fcimb.2020.00001 PMID: 32083019

20. Kraiczy P, Stevenson B. Complement regulator-acquiring surface proteins of *Borrelia burgdorferi*: Structure, function and regulation of gene expression. Ticks and tick-borne diseases. 2013; 4(1–2):26–34. https://doi.org/10.1016/j.ttbdis.2012.10.039 PMID: 23219363

21. Hart T, Nguyen NTT, Nowak NA, Zhang F, Linhardt RJ, Diuk-Wasser M, et al. Polymorphic factor H-binding activity of CspA protects Lyme borreliae from the host complement in feeding ticks to facilitate tick-to-host transmission. PLoS pathogens. 2018; 14(5):e1007106. https://doi.org/10.1371/journal.ppat.1007106 PMID: 29813137

22. Kraiczy P, Hellwage J, Skerka C, Becker H, Kirschfink M, Simon MM, et al. Complement resistance of *Borrelia burgdorferi* correlates with the expression of BbCRASP-1, a novel linear plasmid-encoded surface protein that interacts with human factor H and FHL-1 and is unrelated to Erp proteins. The Journal of biological chemistry. 2004; 279(4):2421–9. https://doi.org/10.1074/jbc.M308343200 PMID: 14607842

23. Bykowski T, Woodman ME, Cooley AE, Brissette CA, Brade V, Wallich R, et al. Coordinated expression of *Borrelia burgdorferi* complement regulator-acquiring surface proteins during the Lyme disease spirochete's mammal-tick infection cycle. Infection and immunity. 2007; 75(9):4227–36. https://doi.org/10.1128/IAI.00604-07 PMID: 17562769

24. Wallich R, Pattathu J, Kitiratschky V, Brenner C, Zipfel PF, Brade V, et al. Identification and functional characterization of complement regulator-acquiring surface protein 1 of the Lyme disease spirochetes *Borrelia afzelii* and *Borrelia garinii*. Infection and immunity. 2005; 73(4):2351–9. https://doi.org/10.1128/IAI.73.4.2351-2359.2005 PMID: 15784581

25. Hammerschmidt C, Koenigs A, Siegel C, Hallstrom T, Skerka C, Wallich R, et al. Versatile roles of CspA orthologs in complement inactivation of serum-resistant Lyme disease spirochetes. Infection and immunity. 2014; 82(1):380–92. https://doi.org/10.1128/IAI.01094-13 PMID: 24191298

26. Marcinkiewicz AL, Dupuis AP 2nd, Zamba-Campero M, Nowak N, Kraiczy P, Ram S, et al. Blood treatment of Lyme borreliae demonstrates the mechanism of CspZ-mediated complement evasion to promote systemic infection in vertebrate hosts. Cellular microbiology. 2019; 21(2):e12998. https://doi.org/10.1111/cmi.12998 PMID: 30571845

27. Isogai E, Tanaka S, Braga IS 3rd, Itakura C, Isogai H, Kimura K, et al. Experimental *Borrelia garinii* infection of Japanese quail. Infection and immunity. 1994; 62(8):3580–2. https://doi.org/10.1128/iai.62.8.3580-3582.1994 PMID: 8039933

28. Frye AM, Hart TM, Tufts DM, Ram S, Diuk-Wasser MA, Kraiczy P, et al. A soft tick *Ornithodoros moubata* salivary protein OmCI is a potent inhibitor to prevent avian complement activation. Ticks and tick-borne diseases. 2020; 11(2):101354. https://doi.org/10.1016/j.ttbdis.2019.101354 PMID: 31866440

29. Hart T, Yang X, Pal U, Lin YP. Identification of Lyme borreliae proteins promoting vertebrate host blood-specific spirochete survival in Ixodes scapularis nymphs using artificial feeding chambers. Ticks and tick-borne diseases. 2018; 9(5):1057–1063. https://doi.org/10.1016/j.ttbdis.2018.03.033 PMID: 29653905

30. Finnie JA, Stewart RB, Aston WP. A comparison of cobra venom factor-induced depletion of serum C3 in eight different strains of mice. Dev Comp Immunol. 1981; 5(4):697–701. https://doi.org/10.1016/s0145-305x(81)80045-6 PMID: 6797851

31. Hallstrom T, Siegel C, Morgelin M, Kraiczy P, Skerka C, Zipfel PF. CspA from *Borrelia burgdorferi* inhibits the terminal complement pathway. mBio. 2013; 4(4):e00481–13. https://doi.org/10.1128/mBio.00481-13 PMID: 23943762

32. Wywial E, Haven J, Casjens SR, Hernandez YA, Singh S, Mongodin EF, et al. Fast, adaptive evolution at a bacterial host-resistance locus: the PFam54 gene array in *Borrelia burgdorferi*. Gene. 2009; 445 (1–2):26–37. https://doi.org/10.1016/j.gene.2009.05.017 PMID: 19505540

33. Qiu WG, Martin CL. Evolutionary genomics of *Borrelia burgdorferi* sensu lato: findings, hypotheses, and the rise of hybrids. Infection, genetics and evolution: journal of molecular epidemiology and evolutionary genetics in infectious diseases. 2014; 27:576–93. https://doi.org/10.1016/j.meegid.2014.03.025 PMID: 24704760

34. Walter KS, Carpi G, Caccone A, Diuk-Wasser MA. Genomic insights into the ancient spread of Lyme disease across North America. Nat Ecol Evol. 2017; 1(10):1569–76. https://doi.org/10.1038/s41559-017-0282-8 PMID: 29185509

35. O'Keeffe KR, Oppler ZJ, Brisson D. Evolutionary ecology of Lyme *Borrelia*. Infection, genetics and evolution: journal of molecular epidemiology and evolutionary genetics in infectious diseases. 2020:104570. https://doi.org/10.1016/j.meegid.2020.104570 PMID: 32998077

36. Kurtenbach K, De Michelis S, Etti S, Schafer SM, Sewell HS, Brade V, et al. Host association of *Borrelia burgdorferi* sensu lato—the key role of host complement. Trends in microbiology. 2002; 10(2):74–9. https://doi.org/10.1016/s0966-842x(01)02298-3 PMID: 11827808

37. Ginsberg HS, Buckley PA, Balmforth MG, Zhioua E, Mitra S, Buckley FG. Reservoir competence of native North American birds for the lyme disease spirochete, *Borrelia burgdorferi*. Journal of medical entomology. 2005; 42(3):445–9. https://doi.org/10.1603/0022-2585(2005)042[0445:RCONNA]2.0.CO;2 PMID: 15962798

38. Heylen D, Adriaensen F, Van Dongen S, Sprong H, Matthysen E. Ecological factors that determine Ixodes ricinus tick burdens in the great tit (*Parus major*), an avian reservoir of *Borrelia burgdorferi* s.l. International journal for parasitology. 2013; 43(8):603–11. https://doi.org/10.1016/j.ijpara.2013.02.007 PMID: 23597868

39. Heylen DJA, Muller W, Vermeulen A, Sprong H, Matthysen E. Virulence of recurrent infestations with *Borrelia*-infected ticks in a *Borrelia*-amplifying bird. Scientific reports. 2015; 5:16150. https://doi.org/10.1038/srep16150 PMID: 26553505

40. Heylen D, Fonville M, van Leeuwen AD, Sprong H. Co-infections and transmission dynamics in a tick-borne bacterium community exposed to songbirds. Environ Microbiol. 2016; 18(3):988–96. https://doi.org/10.1111/1462-2920.13164 PMID: 26627444

41. Heylen DJ, Sprong H, Krawczyk A, Van Houtte N, Genne D, Gomez-Chamorro A, et al. Inefficient co-feeding transmission of *Borrelia afzelii* in two common European songbirds. Scientific reports. 2017; 7:39596. https://doi.org/10.1038/srep39596 PMID: 28054584

42. Norte AC, Lopes de Carvalho I, Nuncio MS, Araujo PM, Matthysen E, Albino Ramos J, et al. Getting under the birds' skin: tissue tropism of *Borrelia burgdorferi* s.l. in naturally and experimentally infected avian hosts. Microb Ecol. 2020; 79(3):756–69. https://doi.org/10.1007/s00248-019-01442-3 PMID: 31612324

43. Norte AC, Costantini D, Araujo PM, Eens M, Ramos JA, Heylen D. Experimental infection by microparasites affects the oxidative balance in their avian reservoir host the blackbird *Turdus merula*. Ticks and tick-borne diseases. 2018; 9(3):720–9. https://doi.org/10.1016/j.ttbdis.2018.02.009 PMID: 29478884

44. Richter D, Spielman A, Komar N, Matuschka FR. Competence of American robins as reservoir hosts for Lyme disease spirochetes. Emerging infectious diseases. 2000; 6(2):133–8. https://doi.org/10.3201/eid0602.000205 PMID: 10756146

45. Piesman J, Dolan MC, Schriefer ME, Burkot TR. Ability of experimentally infected chickens to infect ticks with the Lyme disease spirochete, *Borrelia burgdorferi*. The American journal of tropical medicine and hygiene. 1996; 54(3):294–8. https://doi.org/10.4269/ajtmh.1996.54.294 PMID: 8600769

46. Olsen B, Gylfe A, Bergstrom S. Canary finches (*Serinus canaria*) as an avian infection model for Lyme borreliosis. Microbial pathogenesis. 1996; 20(6):319–24. https://doi.org/10.1006/mpat.1996.0030 PMID: 8831827

47. Burgess EC. Experimental inoculation of mallard ducks (*Anas platyrhynchos platyrhynchos*) with *Borrelia burgdorferi*. Journal of wildlife diseases. 1989; 25(1):99–102. https://doi.org/10.7589/0090-3558-25.1.99 PMID: 2644453

48. Hoogstraal H, Kaiser MN, Traylor MA, Guindy E, Gaber S. Ticks (Ixodidae) on birds migrating from Europe and Asia to Africa 1959–61. Bull World Health Organ. 1963; 28(2):235–62. PMID: 13961632

49. Anderson JF, Magnarelli LA. Epizootiology of Lyme disease-causing borreliae. Clinics in dermatology. 1993; 11(3):339–51. https://doi.org/10.1016/0738-081x(93)90088-t PMID: 8221515

50. Kurtenbach K, Peacey M, Rijpkema SG, Hoodless AN, Nuttall PA, Randolph SE. Differential transmission of the genospecies of *Borrelia burgdorferi* sensu lato by game birds and small rodents in England. Applied and environmental microbiology. 1998; 64(4):1169–74. https://doi.org/10.1128/AEM.64.4.1169-1174.1998 PMID: 9546150

51. Moraru GM, Goddard J, Paddock CD, Varela-Stokes A. Experimental infection of cotton rats and bobwhite quail with *Rickettsia parkeri*. Parasites & vectors. 2013; 6:70. https://doi.org/10.1186/1756-3305-6-70 PMID: 23497681

52. Kurtenbach K, Carey D, Hoodless AN, Nuttall PA, Randolph SE. Competence of pheasants as reservoirs for Lyme disease spirochetes. Journal of medical entomology. 1998; 35(1):77–81. https://doi.org/10.1093/jmedent/35.1.77 PMID: 9542349

53. Kurtenbach K, Sewell HS, Ogden NH, Randolph SE, Nuttall PA. Serum complement sensitivity as a key factor in Lyme disease ecology. Infection and immunity. 1998; 66(3):1248–51. https://doi.org/10.1128/IAI.66.3.1248-1251.1998 PMID: 9488421

54. Bernard Q, Grillon A, Lenormand C, Ehret-Sabatier L, Boulanger N. Skin Interface, a Key Player for *Borrelia* Multiplication and Persistence in Lyme Borreliosis. Trends in parasitology. 2020; 36(3):304–14. https://doi.org/10.1016/j.pt.2019.12.017 PMID: 32007396

55. Strobel L, Johswich KO. Anticoagulants impact on innate immune responses and bacterial survival in whole blood models of *Neisseria meningitidis* infection. Scientific reports. 2018; 8(1):10225. https://doi.org/10.1038/s41598-018-28583-8 PMID: 29977064

56. Mollnes TE, Brekke OL, Fung M, Fure H, Christiansen D, Bergseth G, et al. Essential role of the C5a receptor in E coli-induced oxidative burst and phagocytosis revealed by a novel lepirudin-based human whole blood model of inflammation. Blood. 2002; 100(5):1869–77. PMID: 12176911

57. Logue GL. Effect of heparin on complement activation and lysis of paroxysmal nocturnal hemoglobinuria (PNH) red cells. Blood. 1977; 50(2):239–47. PMID: 17439

58. Pospisilova T, Urbanova V, Hes O, Kopacek P, Hajdusek O, Sima R. Tracking of *Borrelia afzelii* Transmission from Infected *Ixodes ricinus* Nymphs to Mice. Infection and immunity. 2019; 87(6): e00896–18. https://doi.org/10.1128/IAI.00896-18 PMID: 30910791

59. Sertour N, Cotte V, Garnier M, Malandrin L, Ferquel E, Choumet V. Infection Kinetics and Tropism of *Borrelia burgdorferi* sensu lato in Mouse After Natural (via Ticks) or Artificial (Needle) Infection Depends on the Bacterial Strain. Frontiers in microbiology. 2018; 9:1722. https://doi.org/10.3389/fmicb.2018.01722 PMID: 30108573

60. Dolan MC, Piesman J, Mbow ML, Maupin GO, Peter O, Brossard M, et al. Vector competence of *Ixodes scapularis* and *Ixodes ricinus* (Acari: Ixodidae) for three genospecies of Borrelia burgdorferi. Journal of medical entomology. 1998; 35(4):465–70. https://doi.org/10.1093/jmedent/35.4.465 PMID: 9701928

61. Eisen L. Vector competence studies with hard ticks and *Borrelia burgdorferi* sensu lato spirochetes: A review. Ticks and tick-borne diseases. 2020; 11(3):101359. https://doi.org/10.1016/j.ttbdis.2019.101359 PMID: 32067949

62. Rosa PA, Tilly K, Stewart PE. The burgeoning molecular genetics of the Lyme disease spirochaete. Nature reviews Microbiology. 2005; 3(2):129–43. https://doi.org/10.1038/nrmicro1086 PMID: 15685224

63. Lawrenz MB, Wooten RM, Zachary JF, Drouin SM, Weis JJ, Wetsel RA, et al. Effect of complement component C3 deficiency on experimental Lyme borreliosis in mice. Infection and immunity. 2003; 71 (8):4432–40. https://doi.org/10.1128/IAI.71.8.4432-4440.2003 PMID: 12874322

64. van Burgel ND, Balmus NC, Fikrig E, van Dam AP. Infectivity of *Borrelia burgdorferi* sensu lato is unaltered in C3-deficient mice. Ticks and tick-borne diseases. 2011; 2(1):20–6. https://doi.org/10.1016/j.ttbdis.2010.10.003 PMID: 21771533

65. Ricklin D, Reis ES, Lambris JD. Complement in disease: a defence system turning offensive. Nat Rev Nephrol. 2016; 12(7):383–401. https://doi.org/10.1038/nrneph.2016.70 PMID: 27211870

66. Woodman ME, Cooley AE, Miller JC, Lazarus JJ, Tucker K, Bykowski T, et al. *Borrelia burgdorferi* binding of host complement regulator factor H is not required for efficient mammalian infection. Infection and immunity. 2007; 75(6):3131–9. https://doi.org/10.1128/IAI.01923-06 PMID: 17420242

67. Tyson K, Elkins C, Patterson H, Fikrig E, de Silva A. Biochemical and functional characterization of Salp20, an Ixodes scapularis tick salivary protein that inhibits the complement pathway. Insect Mol Biol. 2007; 16(4):469–79. https://doi.org/10.1111/j.1365-2583.2007.00742.x PMID: 17651236

68. Schuijt TJ, Hovius JW, van Burgel ND, Ramamoorthi N, Fikrig E, van Dam AP. The tick salivary protein Salp15 inhibits the killing of serum-sensitive *Borrelia burgdorferi* sensu lato isolates. Infection and immunity. 2008; 76(7):2888–94. https://doi.org/10.1128/IAI.00232-08 PMID: 18426890

69. Schuijt TJ, Coumou J, Narasimhan S, Dai J, Deponte K, Wouters D, et al. A tick mannose-binding lectin inhibitor interferes with the vertebrate complement cascade to enhance transmission of the lyme disease agent. Cell host & microbe. 2011; 10(2):136–46. https://doi.org/10.1016/j.chom.2011.06.010 PMID: 21843870

70. Kraiczy P, Skerka C, Brade V, Zipfel PF. Further characterization of complement regulator-acquiring surface proteins of *Borrelia burgdorferi*. Infection and immunity. 2001; 69(12):7800–9. https://doi.org/10.1128/IAI.69.12.7800-7809.2001 PMID: 11705962

71. Hellwage J, Meri T, Heikkila T, Alitalo A, Panelius J, Lahdenne P, et al. The complement regulator factor H binds to the surface protein OspE of *Borrelia burgdorferi*. The Journal of biological chemistry. 2001; 276(11):8427–35. https://doi.org/10.1074/jbc.M007994200 PMID: 11113124

72. Caine JA, Lin YP, Kessler JR, Sato H, Leong JM, Coburn J. *Borrelia burgdorferi* outer surface protein C (OspC) binds complement component C4b and confers bloodstream survival. Cellular microbiology. 2017. https://doi.org/10.1111/cmi.12786 PMID: 28873507

73. Garcia BL, Zhi H, Wager B, Hook M, Skare JT. *Borrelia burgdorferi* BBK32 Inhibits the Classical Pathway by Blocking Activation of the C1 Complement Complex. PLoS pathogens. 2016; 12(1):e1005404. https://doi.org/10.1371/journal.ppat.1005404 PMID: 26808924

74. Lin YP, Tan X, Caine JA, Castellanos M, Chaconas G, Coburn J, et al. Strain-specific joint invasion and colonization by Lyme disease spirochetes is promoted by outer surface protein C. PLoS pathogens. 2020; 16(5):e1008516. https://doi.org/10.1371/journal.ppat.1008516 PMID: 32413091

75. Lin YP, Benoit V, Yang X, Martinez-Herranz R, Pal U, Leong JM. Strain-specific variation of the decorin-binding adhesin DbpA influences the tissue tropism of the lyme disease spirochete. PLoS pathogens. 2014; 10(7):e1004238. https://doi.org/10.1371/journal.ppat.1004238 PMID: 25079227

76. Brangulis K, Akopjana I, Petrovskis I, Kazaks A, Tars K. Structural analysis of the outer surface proteins from *Borrelia burgdorferi* paralogous gene family 54 that are thought to be the key players in the pathogenesis of Lyme disease. Journal of structural biology. 2020; 210(2):107490. https://doi.org/10.1016/j.jsb.2020.107490 PMID: 32135236

77. Kondrashov FA, Rogozin IB, Wolf YI, Koonin EV. Selection in the evolution of gene duplications. Genome biology. 2002; 3(2):RESEARCH0008. https://doi.org/10.1186/gb-2002-3-2-research0008 PMID: 11864370

78. Hammerschmidt C, Klevenhaus Y, Koenigs A, Hallstrom T, Fingerle V, Skerka C, et al. BGA66 and BGA71 facilitate complement resistance of *Borrelia bavariensis* by inhibiting assembly of the membrane attack complex. Molecular microbiology. 2016; 99(2):407–24. https://doi.org/10.1111/mmi.13239 PMID: 26434356

79. Tkacova Z, Pulzova LB, Mochnacova E, Jimenez-Munguia I, Bhide K, Mertinkova P, et al. Identification of the proteins of *Borrelia garinii* interacting with human brain microvascular endothelial cells. Ticks and tick-borne diseases. 2020; 11(4):101451. https://doi.org/10.1016/j.ttbdis.2020.101451 PMID: 32360026

80. Koenigs A, Hammerschmidt C, Jutras BL, Pogoryelov D, Barthel D, Skerka C, et al. BBA70 of *Borrelia burgdorferi* is a novel plasminogen-binding protein. The Journal of biological chemistry. 2013; 288 (35):25229–43. https://doi.org/10.1074/jbc.M112.413872 PMID: 23861404

81. Lin T, Gao L, Zhang C, Odeh E, Jacobs MB, Coutte L, et al. Analysis of an ordered, comprehensive STM mutant library in infectious *Borrelia burgdorferi*: insights into the genes required for mouse infectivity. PloS one. 2012; 7(10):e47532. https://doi.org/10.1371/journal.pone.0047532 PMID: 23133514

82. Tian W, Skolnick J. How well is enzyme function conserved as a function of pairwise sequence identity? Journal of molecular biology. 2003; 333(4):863–82. https://doi.org/10.1016/j.jmb.2003.08.057 PMID: 14568541

83. Arendt J, Reznick D. Convergence and parallelism reconsidered: what have we learned about the genetics of adaptation? Trends Ecol Evol. 2008; 23(1):26–32. https://doi.org/10.1016/j.tree.2007.09.011 PMID: 18022278

84. Becker NS, Margos G, Blum H, Krebs S, Graf A, Lane RS, et al. Recurrent evolution of host and vector association in bacteria of the *Borrelia burgdorferi* sensu lato species complex. BMC Genomics. 2016; 17(1):734. https://doi.org/10.1186/s12864-016-3016-4 PMID: 27632983

85. Mechai S, Margos G, Feil EJ, Barairo N, Lindsay LR, Michel P, et al. Evidence for Host-Genotype Associations of *Borrelia burgdorferi* Sensu Stricto. PloS one. 2016; 11(2):e0149345. https://doi.org/10.1371/journal.pone.0149345 PMID: 26901761

86. Ogden NH, Feil EJ, Leighton PA, Lindsay LR, Margos G, Mechai S, et al. Evolutionary aspects of emerging Lyme disease in Canada. Applied and environmental microbiology. 2015; 81(21):7350–9. https://doi.org/10.1128/AEM.01671-15 PMID: 26296723

87. Ogden NH, Mechai S, Margos G. Changing geographic ranges of ticks and tick-borne pathogens: drivers, mechanisms and consequences for pathogen diversity. Frontiers in cellular and infection microbiology. 2013; 3:46. https://doi.org/10.3389/fcimb.2013.00046 PMID: 24010124

88. Vollmer SA, Feil EJ, Chu CY, Raper SL, Cao WC, Kurtenbach K, et al. Spatial spread and demographic expansion of Lyme borreliosis spirochaetes in Eurasia. Infection, genetics and evolution: journal of molecular epidemiology and evolutionary genetics in infectious diseases. 2013; 14:147–55. https://doi.org/10.1016/j.meegid.2012.11.014 PMID: 23219915

89. Schulze-Lefert P, Panstruga R. A molecular evolutionary concept connecting nonhost resistance, pathogen host range, and pathogen speciation. Trends Plant Sci. 2011; 16(3):117–25. https://doi.org/10.1016/j.tplants.2011.01.001 PMID: 21317020

90. Huyse T, Poulin R, Theron A. Speciation in parasites: a population genetics approach. Trends in parasitology. 2005; 21(10):469–75. https://doi.org/10.1016/j.pt.2005.08.009 PMID: 16112615

91. Yokoyama Y, Lambeck K, De Deckker P, Johnston P, Fifield LK. Timing of the Last Glacial Maximum from observed sea-level minima. Nature. 2000; 406(6797):713–6. https://doi.org/10.1038/35021035 PMID: 10963593

92. Clark PU, Dyke AS, Shakun JD, Carlson AE, Clark J, Wohlfarth B, et al. The Last Glacial Maximum. Science. 2009; 325(5941):710–4. https://doi.org/10.1126/science.1172873 PMID: 19661421

93. Moller AP, Merino S, Soler JJ, Antonov A, Badas EP, Calero-Torralbo MA, et al. Assessing the effects of climate on host-parasite interactions: a comparative study of European birds and their parasites. PloS one. 2013; 8(12):e82886. https://doi.org/10.1371/journal.pone.0082886 PMID: 24391725

94. Brunner FS, Eizaguirre C. Can environmental change affect host/parasite-mediated speciation? Zoology (Jena). 2016; 119(4):384–94. https://doi.org/10.1016/j.zool.2016.04.001 PMID: 27210289

95. Gehman AM, Hall RJ, Byers JE. Host and parasite thermal ecology jointly determine the effect of climate warming on epidemic dynamics. Proceedings of the National Academy of Sciences of the United States of America. 2018; 115(4):744–9. https://doi.org/10.1073/pnas.1705067115 PMID: 29311324

96. Purser JE, Norris SJ. Correlation between plasmid content and infectivity in *Borrelia burgdorferi*. Proceedings of the National Academy of Sciences of the United States of America. 2000; 97(25):13865–70. https://doi.org/10.1073/pnas.97.25.13865 PMID: 11106398

97. Bunikis I, Kutschan-Bunikis S, Bonde M, Bergstrom S. Multiplex PCR as a tool for validating plasmid content of *Borrelia burgdorferi*. Journal of microbiological methods. 2011; 86(2):243–7. https://doi.org/10.1016/j.mimet.2011.05.004 PMID: 21605603

98. Kern A, Zhou CW, Jia F, Xu Q, Hu LT. Live-vaccinia virus encapsulation in pH-sensitive polymer increases safety of a reservoir-targeted Lyme disease vaccine by targeting gastrointestinal release. Vaccine. 2016; 34(38):4507–13. https://doi.org/10.1016/j.vaccine.2016.07.059 PMID: 27502570

99. Coleman AS, Yang X, Kumar M, Zhang X, Promnares K, Shroder D, et al. Borrelia burgdorferi complement regulator-acquiring surface protein 2 does not contribute to complement resistance or host infectivity. PloS one. 2008; 3(8):3010e. https://doi.org/10.1371/journal.pone.0003010 PMID: 18714378

100. Derdakova M, Dudioak V, Brei B, Brownstein JS, Schwartz I, Fish D. Interaction and transmission of two *Borrelia burgdorferi* sensu stricto strains in a tick-rodent maintenance system. Applied and environmental microbiology. 2004; 70(11):6783–8. https://doi.org/10.1128/AEM.70.11.6783-6788.2004 PMID: 15528545

101. Rynkiewicz EC, Brown J, Tufts DM, Huang CI, Kampen H, Bent SJ, et al. Closely-related *Borrelia burgdorferi* (sensu stricto) strains exhibit similar fitness in single infections and asymmetric competition in multiple infections. Parasites & vectors. 2017; 10(1):64. https://doi.org/10.1186/s13071-016-1964-9 PMID: 28166814

102. Altschul SF, Gish W, Miller W, Myers EW, Lipman DJ. Basic local alignment search tool. Journal of molecular biology. 1990; 215(3):403–10. https://doi.org/10.1016/S0022-2836(05)80360-2 PMID: 2231712

103. Notredame C, Higgins DG, Heringa J. T-Coffee: A novel method for fast and accurate multiple sequence alignment. Journal of molecular biology. 2000; 302(1):205–17. https://doi.org/10.1006/jmbi.2000.4042 PMID: 10964570

104. Abascal F, Zardoya R, Telford MJ. TranslatorX: multiple alignment of nucleotide sequences guided by amino acid translations. Nucleic acids research. 2010; 38(Web Server issue):W7–13. https://doi.org/10.1093/nar/gkq291 PMID: 20435676

105. Madeira F, Park YM, Lee J, Buso N, Gur T, Madhusoodanan N, et al. The EMBL-EBI search and sequence analysis tools APIs in 2019. Nucleic acids research. 2019; 47(W1):W636–W41. https://doi.org/10.1093/nar/gkz268 PMID: 30976793

106. Lin YP, Greenwood A, Nicholson LK, Sharma Y, McDonough SP, Chang YF. Fibronectin binds to and induces conformational change in a disordered region of leptospiral immunoglobulin-like protein B. The Journal of biological chemistry. 2009; 284(35):23547–57. https://doi.org/10.1074/jbc.M109.031369 PMID: 19581300

107. Benoit VM, Fischer JR, Lin YP, Parveen N, Leong JM. Allelic variation of the Lyme disease spirochete adhesin DbpA influences spirochetal binding to decorin, dermatan sulfate, and mammalian cells. Infection and immunity. 2011; 79(9):3501–9. https://doi.org/10.1128/IAI.00163-11 PMID: 21708995

108. Suchard MA, Lemey P, Baele G, Ayres DL, Drummond AJ, Rambaut A. Bayesian phylogenetic and phylodynamic data integration using BEAST 1.10. Virus Evol. 2018; 4(1):vey016. https://doi.org/10.1093/ve/vey016 PMID: 29942656

109. Rambaut A. FigTree GitHub repository [Available from: http://tree.bio.ed.ac.uk/software/figtree/.

110. Maddison WP, Maddison D.R. Mesquite: a modular system for evolutionary analysis. Version 3.61 2019 [Available from: http://www.mesquiteproject.org.

111. Kishino H, Hasegawa M. Evaluation of the maximum likelihood estimate of the evolutionary tree topologies from DNA sequence data, and the branching order in hominoidea. J Mol Evol. 1989; 29(2):170–9. https://doi.org/10.1007/BF02100115 PMID: 2509717

112. Shimodaira H, Hasegawa, M. Multiple Comparisons of Log-Likelihoods with Applications to Phylogenetic Inference. Molecular Biology and Evolution. 1999; 16(8):1114.

113. Strimmer K, Rambaut A. Inferring confidence sets of possibly misspecified gene trees. Proc Biol Sci. 2002; 269(1487):137–42. https://doi.org/10.1098/rspb.2001.1862 PMID: 11798428

114. Shimodaira H. An approximately unbiased test of phylogenetic tree selection. Syst Biol. 2002; 51(3):492–508. https://doi.org/10.1080/10635150290069913 PMID: 12079646

115. Wallace IM, O'Sullivan O, Higgins DG, Notredame C. M-Coffee: combining multiple sequence alignment methods with T-Coffee. Nucleic acids research. 2006; 34(6):1692–9. https://doi.org/10.1093/nar/gkl091 PMID: 16556910

116. Nguyen LT, Schmidt HA, von Haeseler A, Minh BQ. IQ-TREE: a fast and effective stochastic algorithm for estimating maximum-likelihood phylogenies. Mol Biol Evol. 2015; 32(1):268–74. https://doi.org/10.1093/molbev/msu300 PMID: 25371430

117. Kalyaanamoorthy S, Minh BQ, Wong TKF, von Haeseler A, Jermiin LS. ModelFinder: fast model selection for accurate phylogenetic estimates. Nature methods. 2017; 14(6):587–9. https://doi.org/10.1038/nmeth.4285 PMID: 28481363

118. Hoang DT, Chernomor O, von Haeseler A, Minh BQ, Vinh LS. UFBoot2: Improving the Ultrafast Bootstrap Approximation. Mol Biol Evol. 2018; 35(2):518–22. https://doi.org/10.1093/molbev/msx281 PMID: 29077904

119. Guindon S, Dufayard JF, Lefort V, Anisimova M, Hordijk W, Gascuel O. New algorithms and methods to estimate maximum-likelihood phylogenies: assessing the performance of PhyML 3.0. Syst Biol. 2010; 59(3):307–21. https://doi.org/10.1093/sysbio/syq010 PMID: 20525638

120. Benjamini YK, A. M. Yekutieli D. Adaptive linear step-up procedures that control the false discovery rate. Biometrika. 2006; 93:491–507.